

Foundation of Synchrotron and Storage Ring

Jie Gao

Institute of High Energy Physics

International school for Accelerator foundation

November 26-30, 2018 Hiroshima University, Japan

Introdcution and Historical Recalls

Charged Particle Dynamics

Relative velocity

$$\beta = v/c,$$

Lorentz factor

$$\gamma = \frac{1}{\sqrt{1 - \beta^2}},$$

Momentum

$$\vec{p} = \gamma m \vec{v},$$

Energy

$$E = \gamma mc^2 = \sqrt{c^2 p^2 + m^2 c^4} = cp/\beta.$$

Equation of motion

$$\frac{d\vec{p}}{dt} = e(\vec{E} + \frac{\vec{v}}{c} \times \vec{B}), \quad \text{Lorentz force}$$

Energy gain

$$\frac{dE}{dt} = e\vec{v} \cdot \vec{E}.$$

$$\begin{aligned} \vec{E} &= -\nabla \phi - \frac{1}{c} \frac{\partial \vec{A}}{\partial t} \\ \vec{B} &= \nabla \times \vec{A} \end{aligned}$$

What is Particle Accelerators and What They are used for?

Accelerator accelerate charged particles by using electric fields both **electrostatic electric field** (DC) and **alternating electric** (RF) field

The direction of the motion of charged particles can be controlled both **electric** or **magnetic** fields

The motion of the charged particle should be **stable** during the acceleration or storage in the accelerator

Accelerators are used in nuclear physics, high energy physics, synchrotron radiation lights for scientific studies, industry and medical...

History of Storage Ring and Colliders

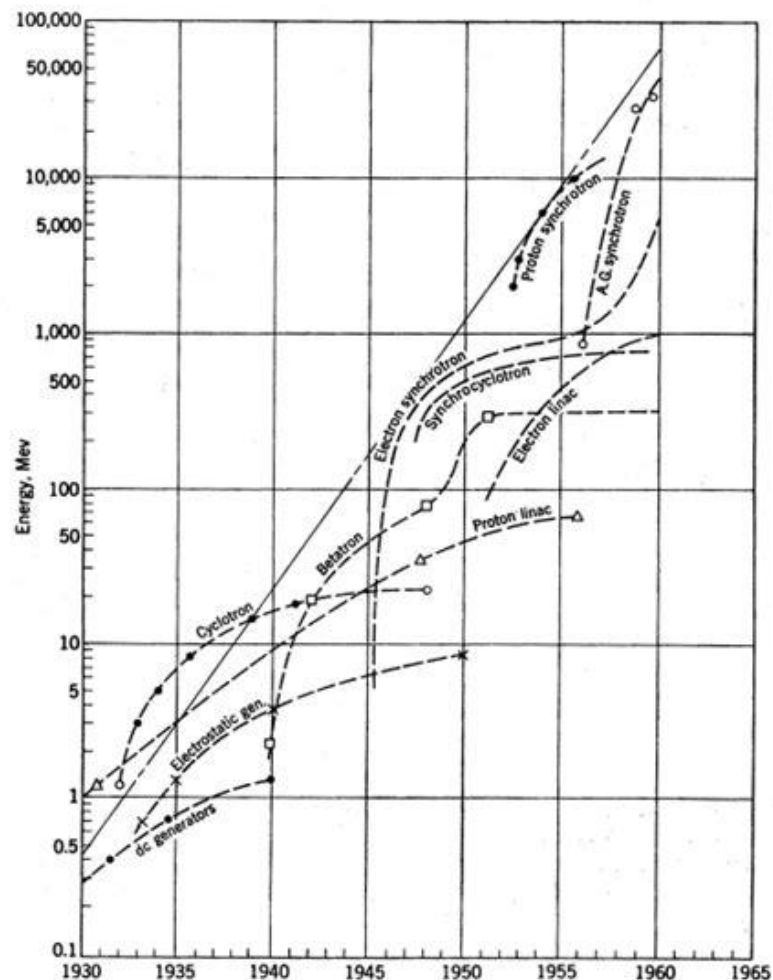
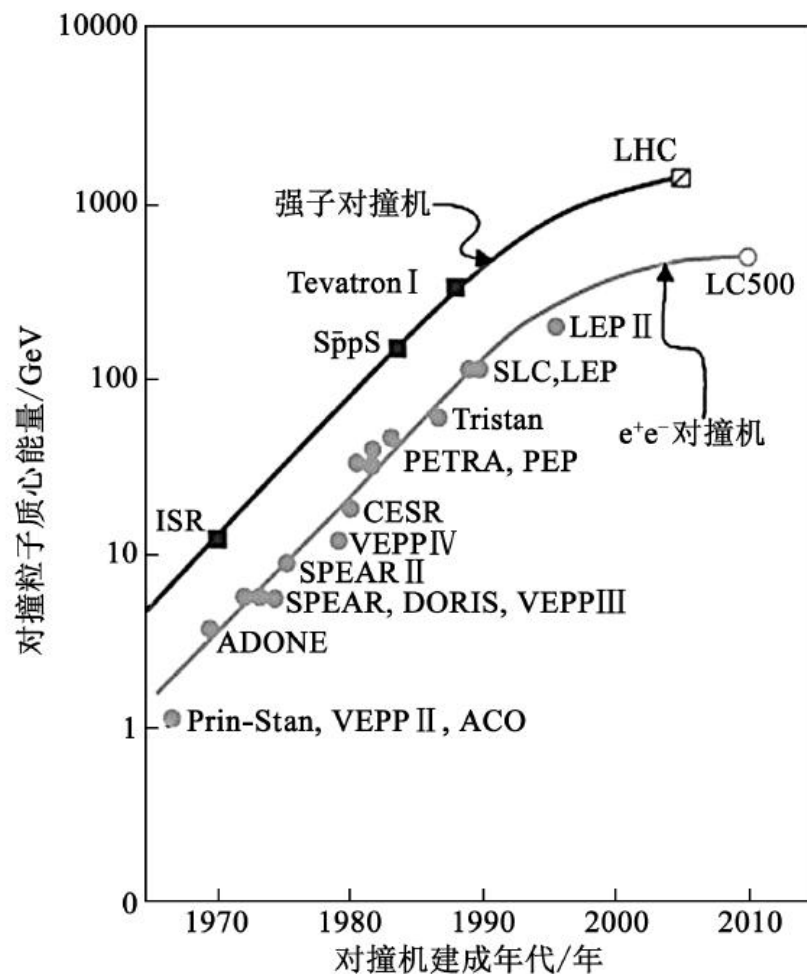


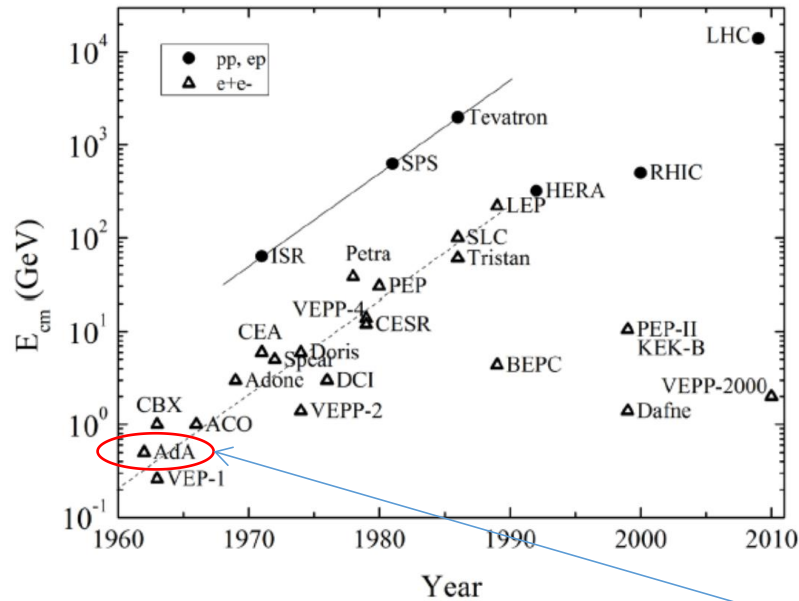
Fig. 1-1. Energies achieved by accelerators from 1930 to 1960. The linear envelope of the individual curves shows an average tenfold increase in energy every six years.

Livingston's curve

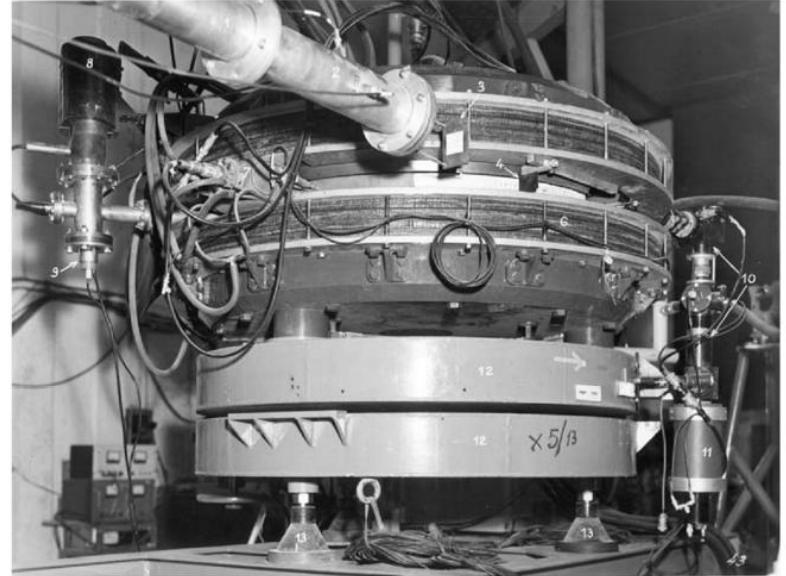


Extended Livingston's curve

Ada: First electron-positron Collider

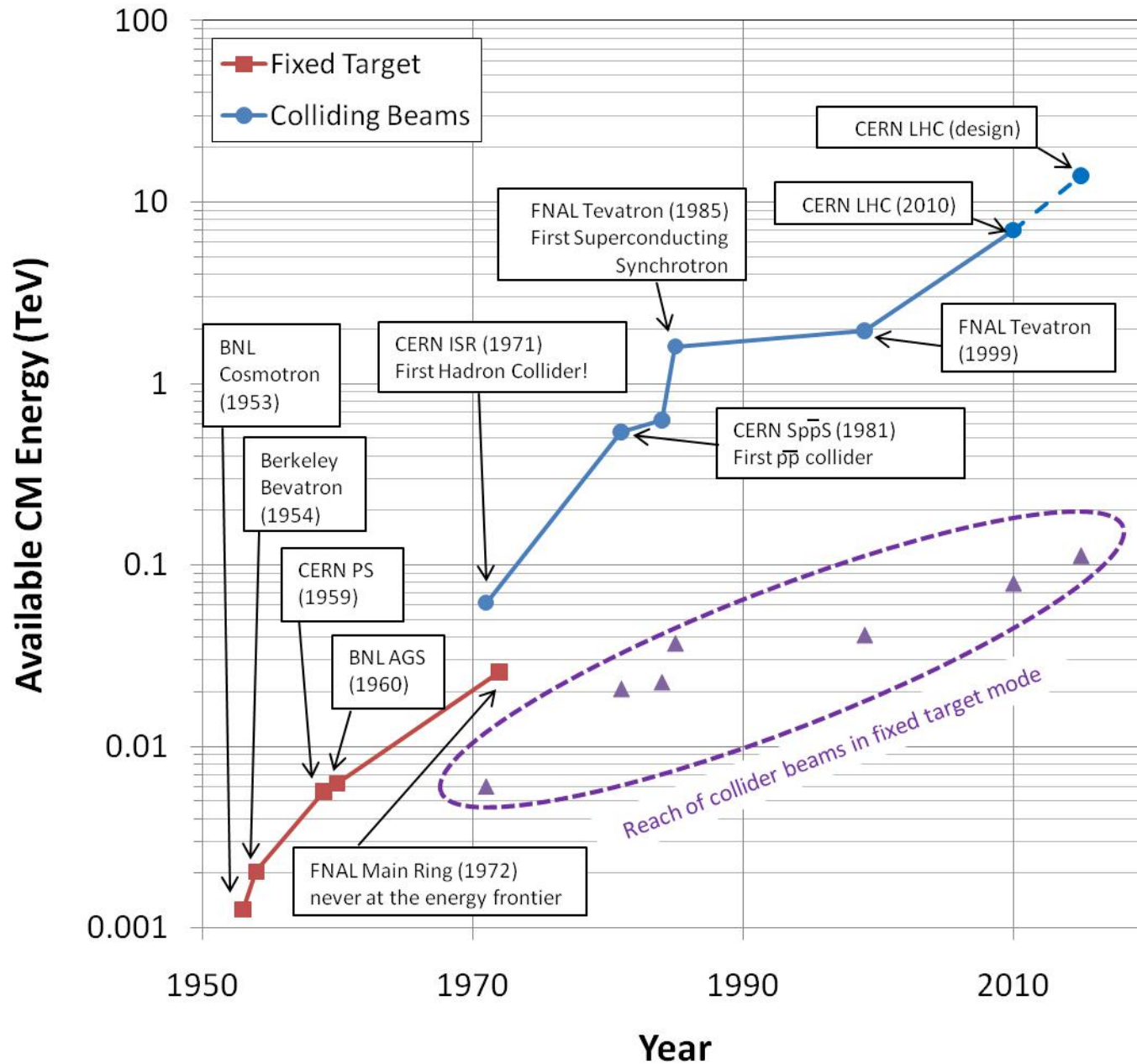


V. Shiltsev,
Physics-Uspekhi, 2012



Ada: 1963 INFN/LAL

Evolution of the Energy Frontier (hadron)



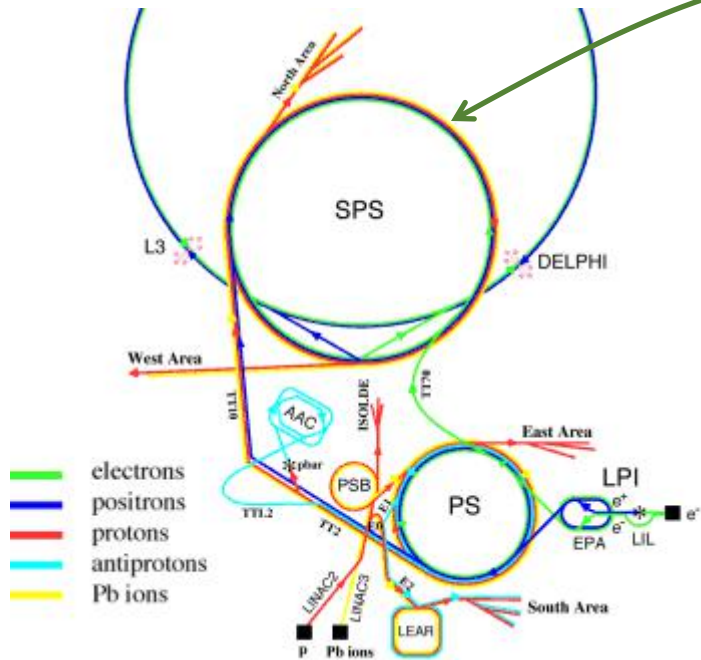
~a factor of 10
every 15 years

History: CERN Intersecting Storage Rings (ISR)



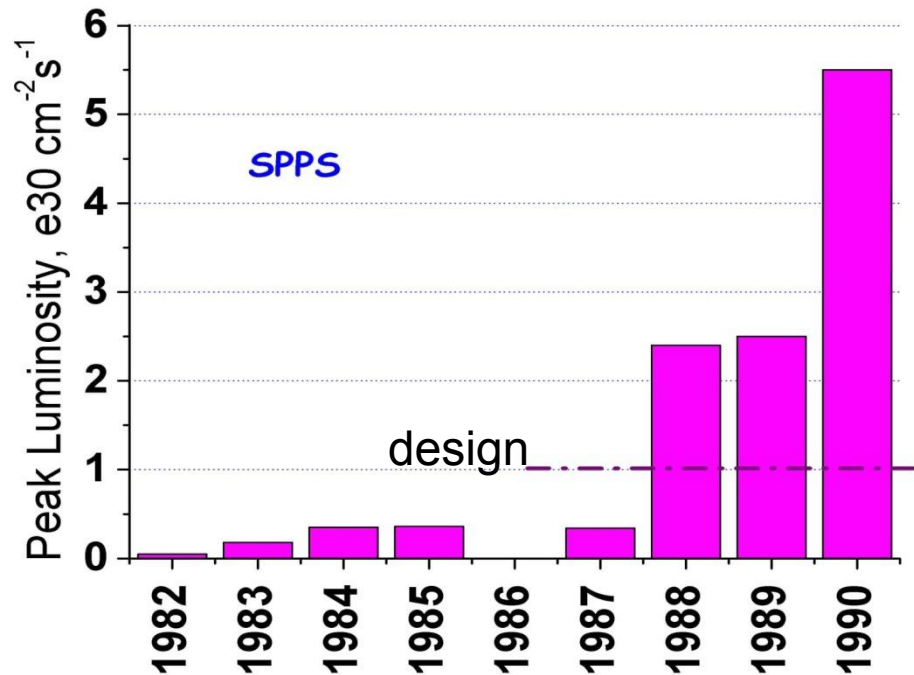
- First hadron collider (p-p)
- Highest CM Energy for 10 years
 - Until SppS
- Reached its design luminosity within the first year.
 - Increased it by a factor of 28 over the next 10 years
- Its peak luminosity in 1982 was $140 \times 10^{30} \text{ cm}^{-2}\text{s}^{-1}$
 - a record that was not broken for 23 years!!

SppS: First proton-antiproton Collider

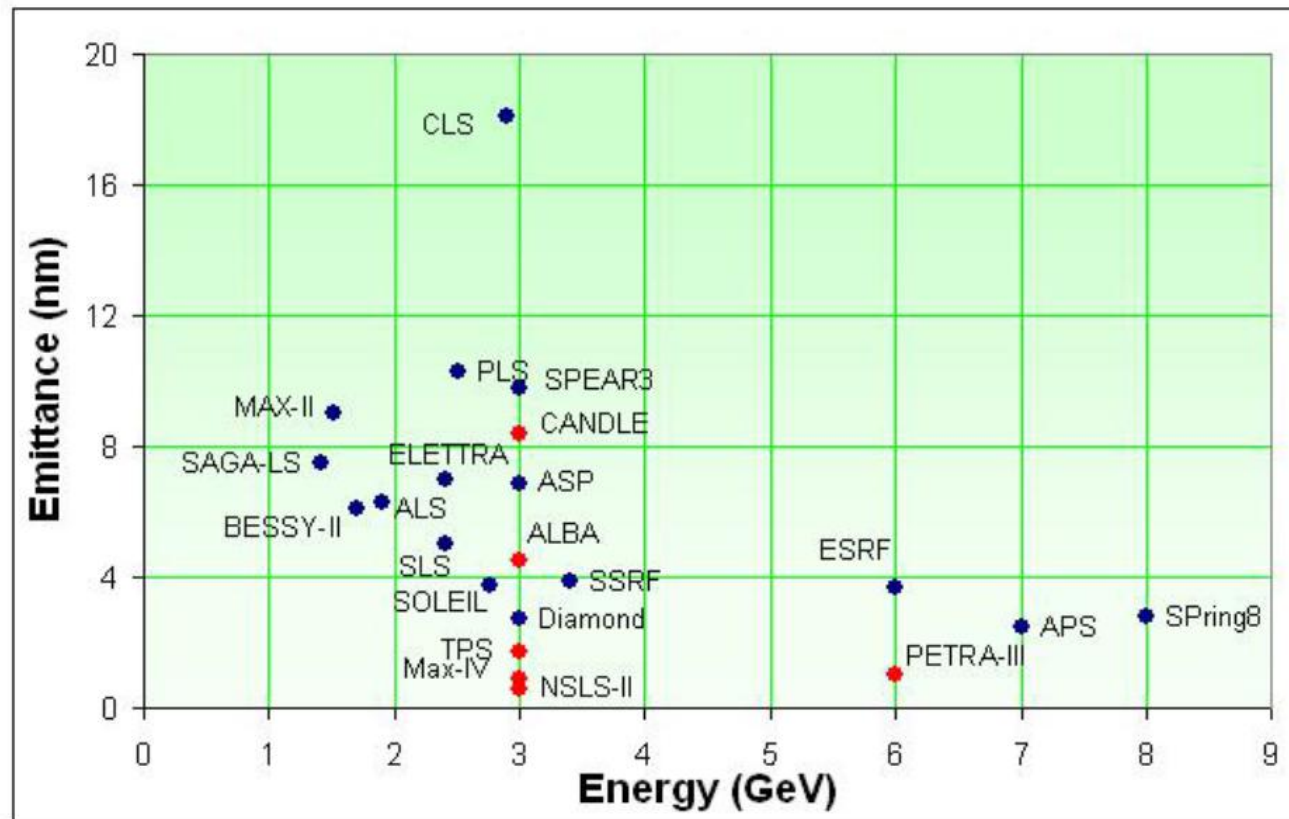


- Protons from the SPS were used to produce antiprotons, which were collected
- These were injected in the opposite direction and accelerated
- First collisions in 1981
- Discovery of W and Z in 1983
 - Nobel Prize for Rubbia and Van der Meer

- Energy initially 270+270 GeV
- Raised to 315+315 GeV
 - Limited by power loss in magnets!
- Peak luminosity: $5.5 \times 10^{30} \text{ cm}^{-2} \text{ s}^{-1}$
 - ~.2% of current LHC



History of Evolution of Synchrotron Radiation Storage Rings



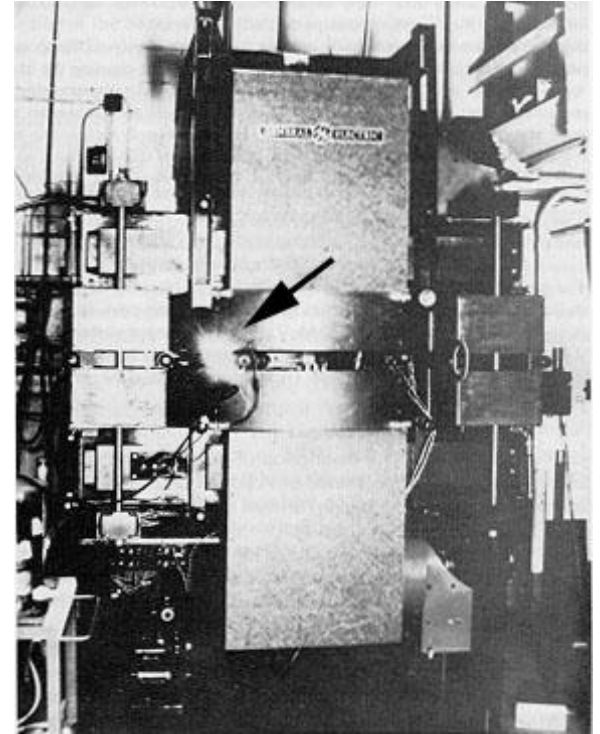
Courtesy of R. Bartolini, Low Emittance Rings Workshop, 2010, CERN

History of Discovery of Synchrotron Radiation

Advances on another accelerator front led to the 1947 **visual observation of synchrotron radiation at GE.**

At GE, Pollack got permission to assemble a team to build a 70-MeV electron synchrotron to test the idea. Fortunately for the future of synchrotron radiation, the machine was not fully shielded and the coating on the doughnut-shaped electron tube was transparent, which allowed a technician to look around the shielding with a large mirror to check for sparking in the tube. Instead, he saw a bright arc of light, which the GE group quickly realized was actually coming from the electron beam. Langmuir is credited as recognizing it as synchrotron radiation or, as he called it, "Schwinger radiation." Subsequent measurements by the GE group began the experimental establishment of its spectral and polarization properties. Characterization measurements were also carried out in the 1950s at a 250-MeV synchrotron at the Lebedev Institute in Moscow.

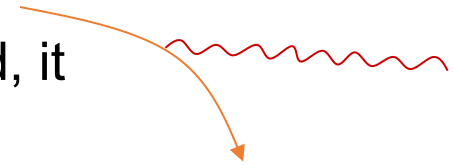
By Arthur L. Robinson



Synchrotron light from the 70-MeV electron synchrotron at GE

Synchrotron Radiation and a Curse

As the trajectory of a charged particle is deflected, it emits “synchrotron radiation”



Radius of curvature

$$P = \frac{1}{6\pi\epsilon_0} \frac{e^2 c}{\rho^2} \left(\frac{E}{m} \right)^4$$

An electron will radiate about 10^{13} times more power than a proton of the same energy!!!!

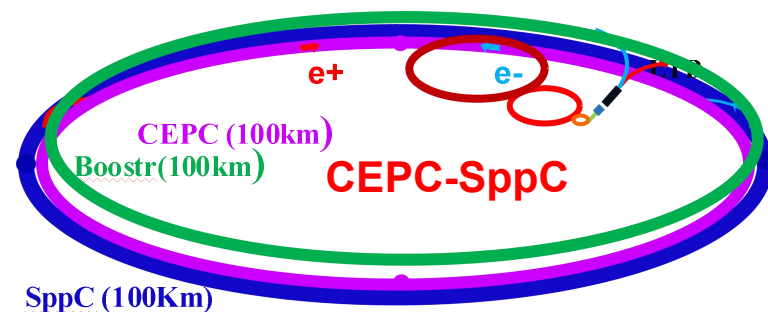
- **Protons:** Synchrotron radiation does not affect kinematics very much
- **Electrons:** Beyond a few MeV, synchrotron radiation becomes very important, and by a few GeV, it dominates kinematics
 - Good Effects:
 - Naturally “cools” beam in all dimensions
 - Basis for light sources, FEL’s, etc.
 - Bad Effects:
 - Beam pipe heating
 - Exacerbates beam-beam effects
 - **Energy loss ultimately limits circular accelerators**

Practical Consequences of Synchrotron Radiation

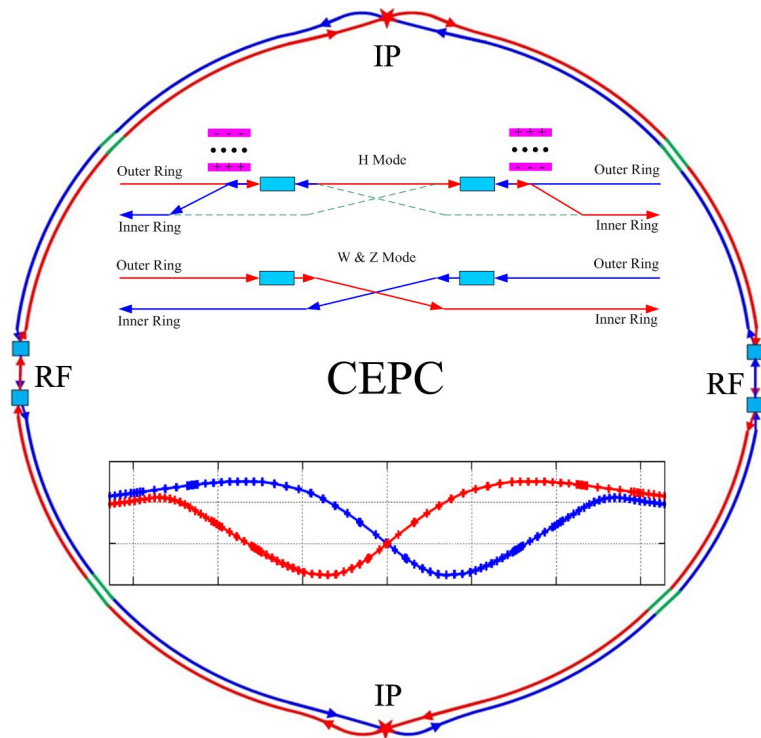
- Proton accelerators
 - Synchrotron radiation not an issue to first order
 - Energy limited by the maximum feasible size and magnetic field.
- Electron accelerators
 - To keep power loss constant, radius must go up as the *square* of the energy ($B \propto 1/E \Rightarrow$ weak magnets, BIG rings):
 - The LHC tunnel was built for LEP, and e^+e^- collider which used the 27 km tunnel to contain 100 GeV beams (1/70th of the LHC energy!!)
 - Beyond CEPC energy, circular synchrotrons have no advantage for e^+e^-
 - -> Linear Collider (a bit more about that later)
- What about muons?
 - Point-like, but heavier than electrons
 - Unstable particle
- Since the beginning, the energy frontier has belonged to proton (and/or antiproton) machines, say later SppC

Paths to the Energy Frontier

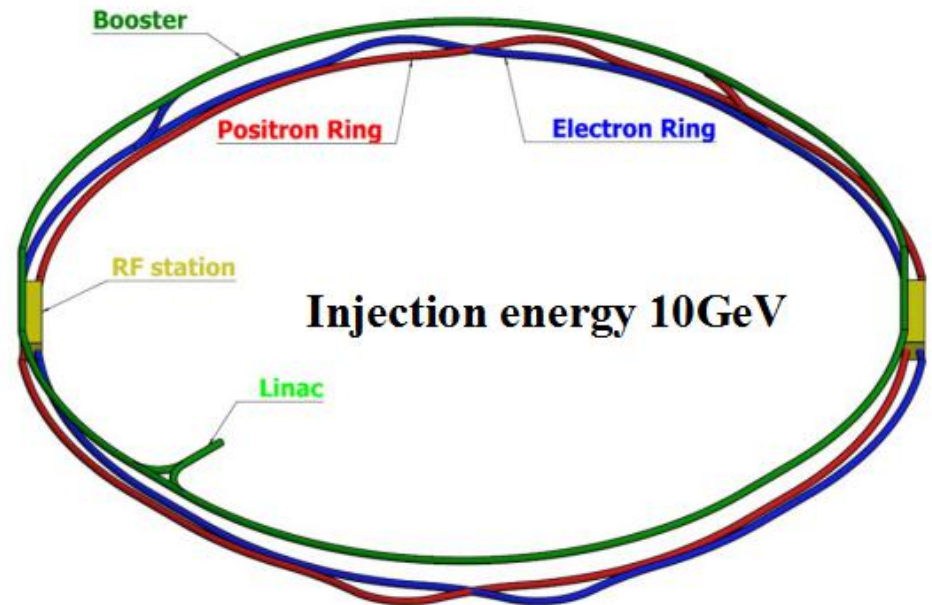
- Leptons vs. Hadrons revisited
 - Because 100% of the beam energy is available to the reaction, a lepton collider is competitive with a hadron collider of ~ 5 -10 times the beam energy (depending on the physics).
 - A lepton collider of >1 TeV/beam could compete with the discovery potential of the LHC
 - LEP reached 100 GeV/beam with a 27 km circumference !
 - Next e^+e^- collider will be large circumference ring (CEPC-SppC) and linear (ILC)



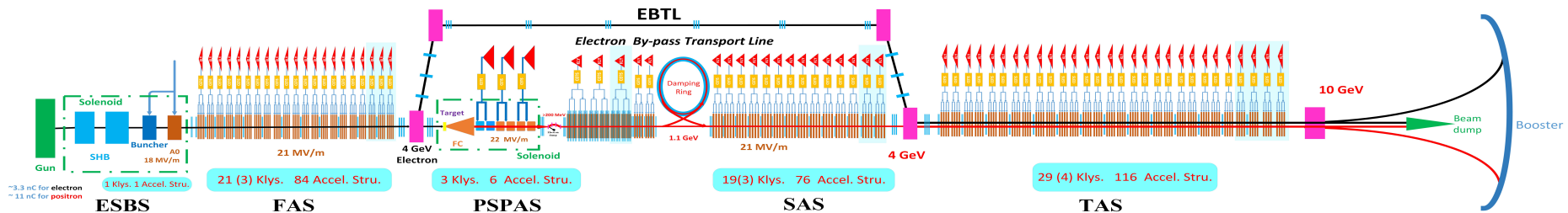
Next Generation Electron-Positron Circular Collider : CEPC CDR Layout (~2030)



CEPC collider ring (100km)



CEPC booster ring (100km)



CEPC Linac injector (1.2km, 10GeV)

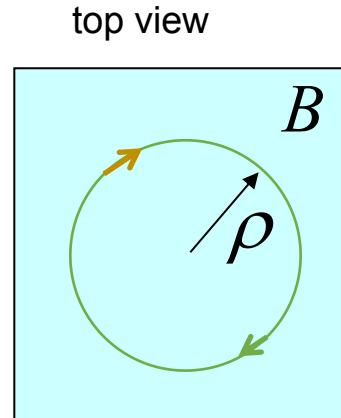
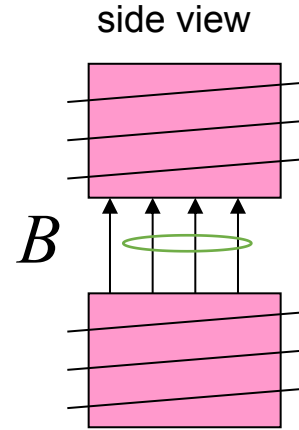
The Cyclotron (1930's)

- A charged particle in a uniform magnetic field will follow a circular path of radius

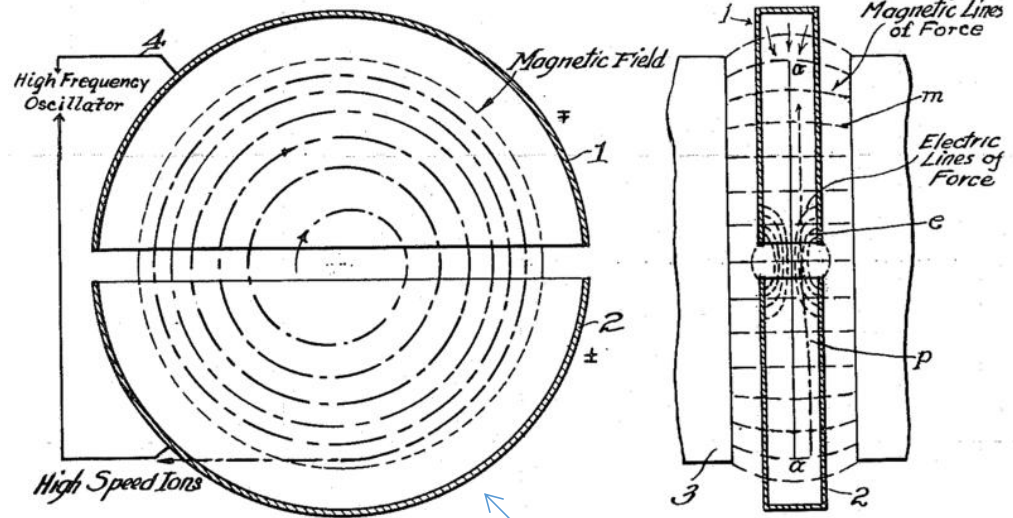
$$\begin{aligned}\rho &= \frac{mv}{qB} \\ f &= \frac{v}{2\pi\rho} \\ &= \frac{qB}{2\pi m} \text{ (constant!!)} \\ \Omega_s &= \frac{f}{2\pi} = \frac{qB}{m}\end{aligned}$$

For a proton:

$$f_C = 15.2 \times B[T] \text{ MHz}$$

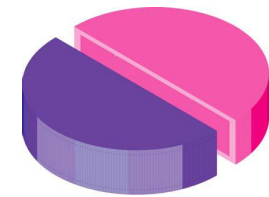


“Cyclotron Frequency”



Accelerating “DEES”

Cyclotron (weak focusing)



- Cyclotrons relied on the fact that magnetic fields between two pole faces are always focusing
- Beam size grows with energy
- The highest energy limited
- Berkeley Bevatron, which had a kinetic energy of 6 GeV
 - High enough to make antiprotons (and win a Nobel Prize)
 - It had an aperture 12"x48"!

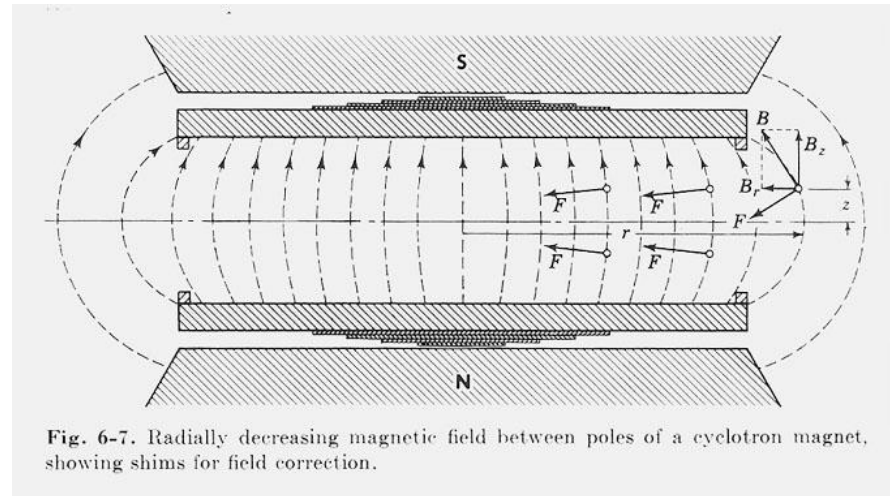
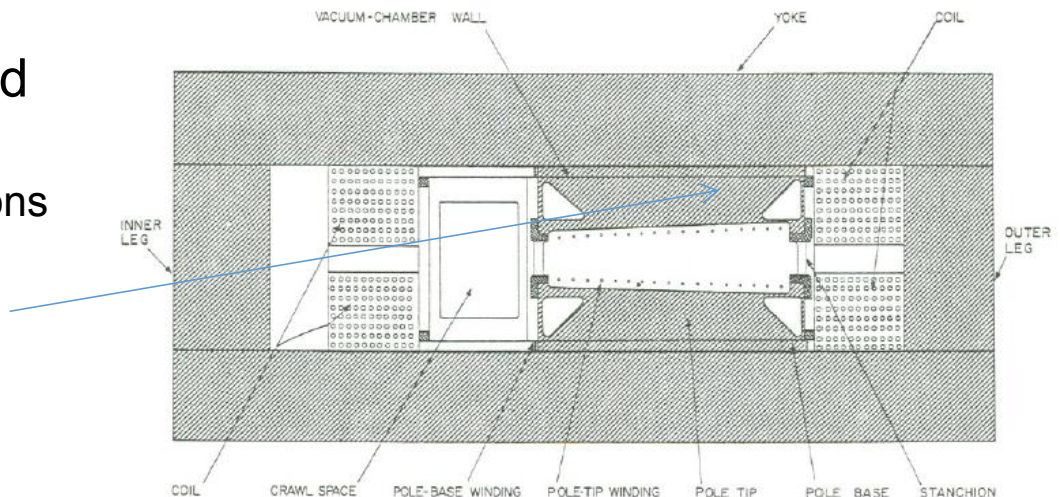
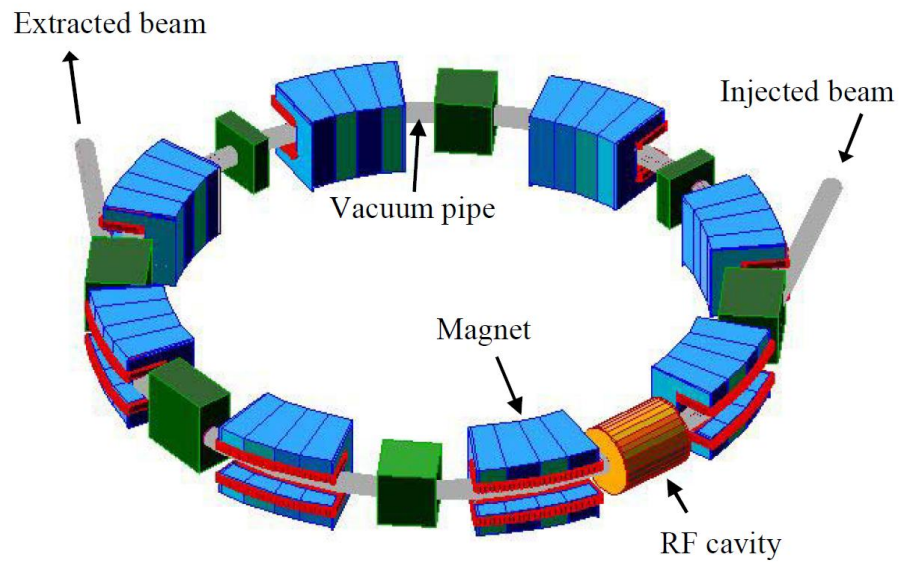


Fig. 6-7. Radially decreasing magnetic field between poles of a cyclotron magnet, showing shims for field correction.



Synchrotron (strong focusing)

- Strong focusing utilizes alternating magnetic gradients to precisely control the focusing of a beam of particles
 - The principle was first developed in 1949 by Nicholas Christophilos, a Greek-American engineer, who was working for an elevator company in Athens at the time.
 - Rather than publish the idea, he applied for a patent, and it went largely ignored.
 - The idea was independently invented in 1952 by Courant, Livingston and Snyder, who later acknowledged the priority of Christophilos' work.
- Although the technique was originally formulated in terms of magnetic gradients, it's much easier to understand in terms of the separate functions of dipole and quadrupole magnets.



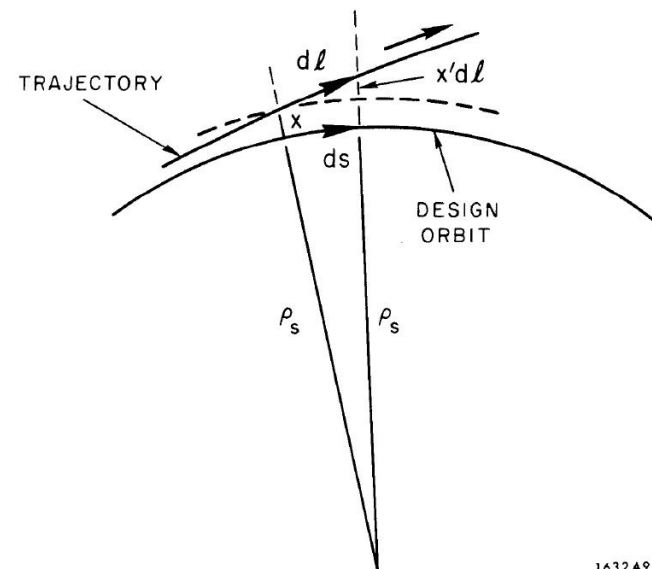
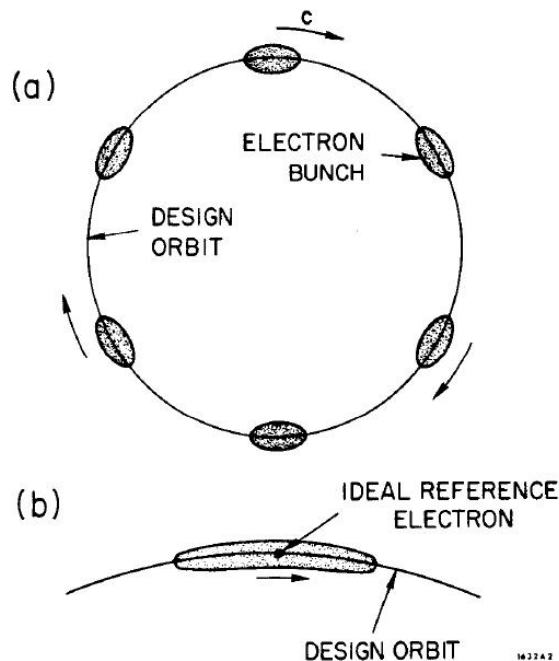
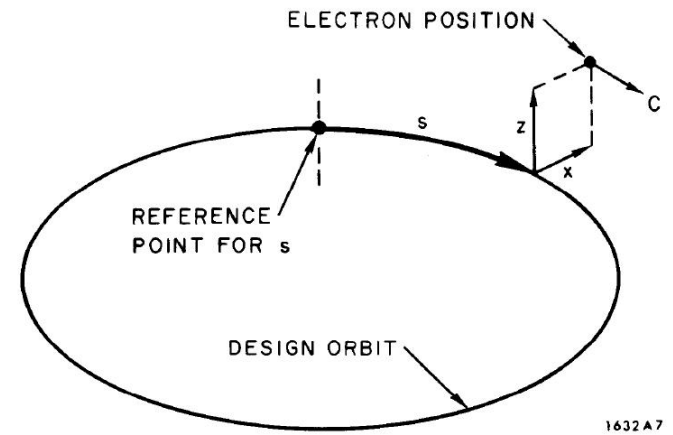
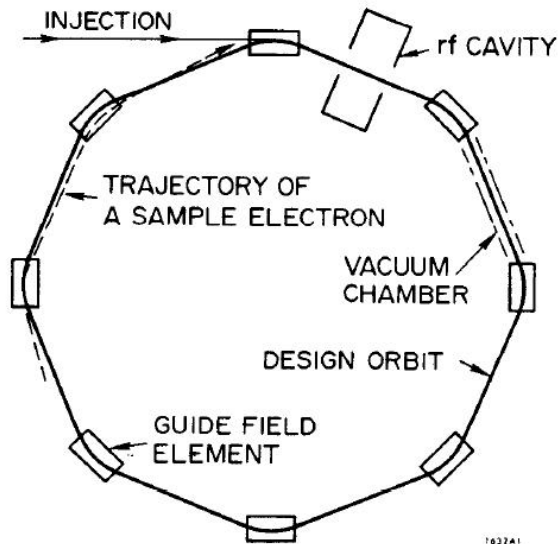
Synchrotron



Two ring e^+e^- collider:
BEPC-II, IHEP, CAS

Single Particle and Linear Dynamics in Storage Ring and Colliders

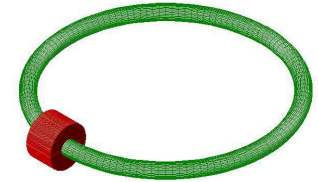
Synchrotron and Storage Ring Dynamics



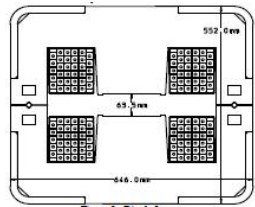
Synchrotron (strong focusing)

- The relativistic form of Newton's Laws for a particle in a magnetic field is:

$$\vec{F} = \frac{d\vec{p}}{dt} = q(\vec{v} \times \vec{B})$$



- A particle in a uniform magnetic field will move in a circle of radius



$$\rho = \frac{p}{qB}$$

\Rightarrow

$$\rho[\text{m}] \approx \frac{p[\text{MeV}/c] / 300}{B[\text{T}]}$$

$$B(\vec{x}, t) \propto p(t)$$

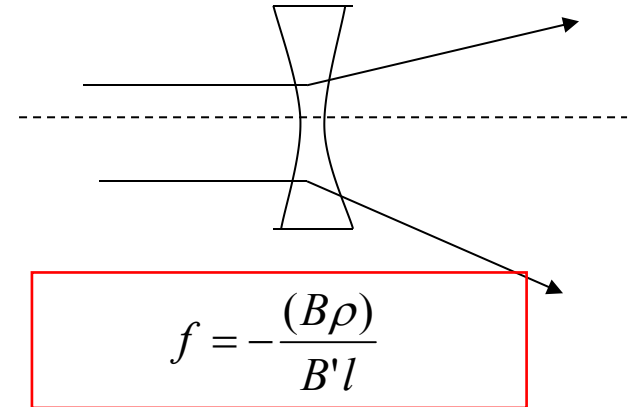
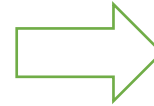
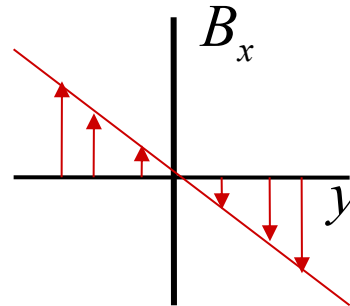
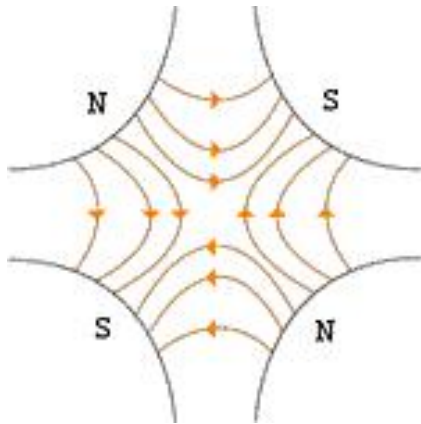
- In a “synchrotron”, the magnetic fields are varied as the beam accelerates such that at all points, and beam motion can be analyzed in a momentum independent way.
- It is usual to talk about the beam “stiffness” in T-m

$$(B\rho) = \frac{p}{q} \Rightarrow (B\rho) [\text{Tm}] \approx \frac{p[\text{MeV}/c]}{300}$$

Booster: $(B\rho) \sim 30 \text{ Tm}$
LHC : $(B\rho) \sim 23000 \text{ Tm}$

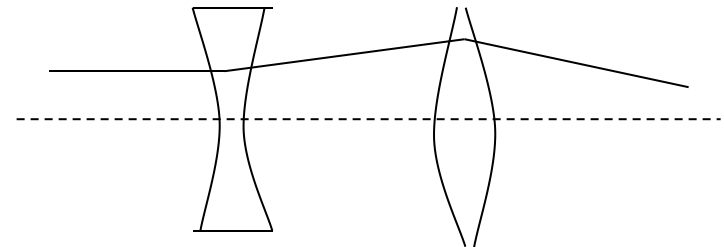
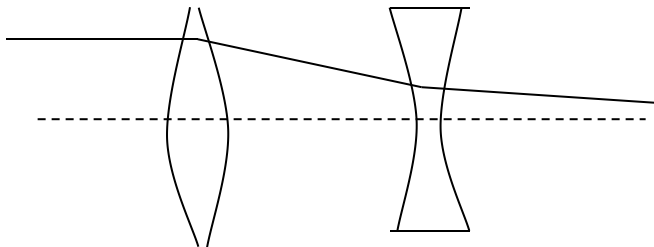
- Thus if at all points $B(\vec{x}, t) \propto p(t)$, then the local bend radius (and therefore the trajectory) will remain constant.

Using Focusing and Defocusing Magnets



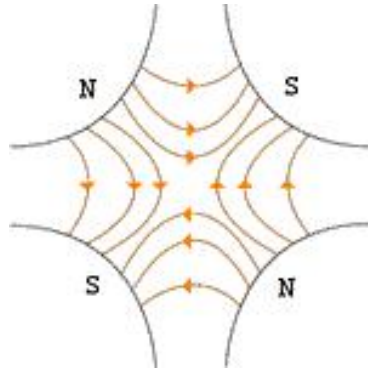
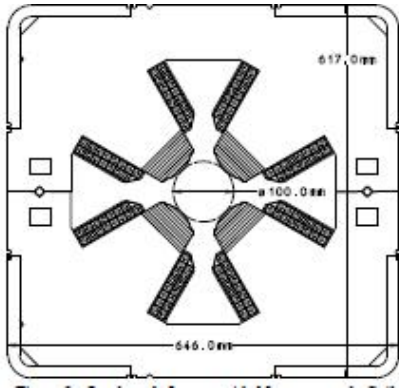
Defocusing!

If we place equal and opposite pairs of lenses, there will be a net focusing regardless of the order



Pairs give net focusing in both planes -> "FODO cell"

Focusing Strength of a Quadrupole



- We can define a focusing strength k by

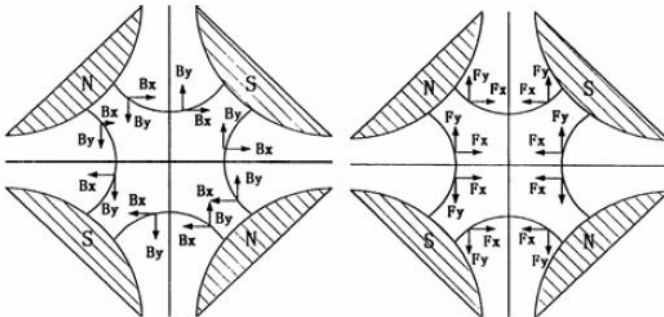
$$k[m^{-2}] = 0.2998 \frac{g[Tesla/m]}{\beta E[GeV]}$$

where, g is the field gradient of the quadrupole magnet.

- The focal length of the quadrupole is given by k as:

$$\frac{1}{f} = kl$$

where l is the path length of the particle in the magnet.



Transvers Motion including both Dipole and Quadrupole (differential equations)

- The equation of motion in the approximation of linear beam dynamics is:

$$x'' + \left(\frac{1}{\rho^2} + k \right) x = 0$$

$$y'' - ky = 0$$

- The term $1/\rho^2$ comes from the fact that dipole magnet field also has a focusing action in the horizontal direction.

- This equation can be generalized as:

$$u'' + Ku = 0 \quad u \text{ represents } x \text{ or } y$$

If K is constant, this is a harmonic oscillator and principal solutions are expressed in matrix formulation:

$$\begin{bmatrix} u(s) \\ u'(s) \end{bmatrix} = \begin{bmatrix} C(s) & S(s) \\ C'(s) & S'(s) \end{bmatrix} \begin{bmatrix} u_0 \\ u'_0 \end{bmatrix}$$

- In a drift space where there is no magnet this matrix is expressed by

$$\begin{bmatrix} u(s) \\ u'(s) \end{bmatrix} = \begin{bmatrix} 1 & s - s_0 \\ 0 & 1 \end{bmatrix} \begin{bmatrix} u_0 \\ u'_0 \end{bmatrix}$$

- In a quadrupole magnet the matrix for focusing case is:

$$\begin{bmatrix} u(s) \\ u'(s) \end{bmatrix} = \begin{bmatrix} \cos \psi & \frac{1}{\sqrt{k_0}} \sin \psi \\ -\sqrt{k_0} \sin \psi & \cos \psi \end{bmatrix} \begin{bmatrix} u_0 \\ u'_0 \end{bmatrix}$$

where

$$\psi = \sqrt{k_0}(s - s_0)$$

- In the plane of defocusing case, we get

$$\begin{bmatrix} u(s) \\ u'(s) \end{bmatrix} = \begin{bmatrix} \cosh \psi & \frac{1}{\sqrt{|k_0|}} \sinh \psi \\ \sqrt{|k_0|} \sinh \psi & \cosh \psi \end{bmatrix} \begin{bmatrix} u_0 \\ u'_0 \end{bmatrix}$$

- If the length of the magnet l is much smaller than the focal length, we may use the so called thin-lens approximation. In this approximation, we set

$$l \rightarrow 0 ,$$

while keeping the focal strength f constant,

$$f^{-1} = k_0 l = \text{const.}$$

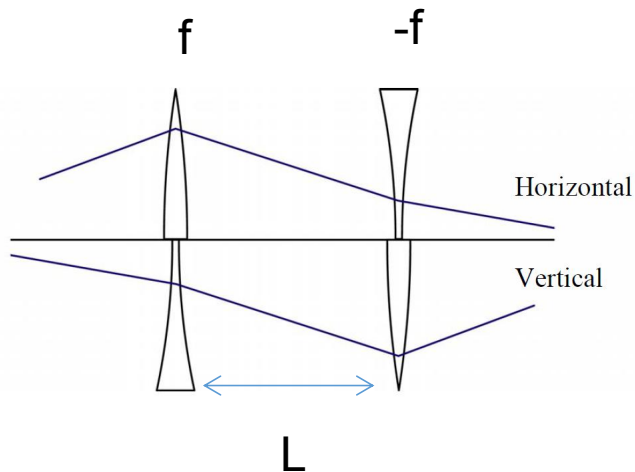
as a consequence,

$$\varphi = \sqrt{k_0} l \rightarrow 0$$

and matrices can be written as,

$$\begin{bmatrix} u \\ u' \end{bmatrix} = \begin{bmatrix} 1 & 0 \\ -\frac{1}{f} & 1 \end{bmatrix} \begin{bmatrix} u_0 \\ u'_0 \end{bmatrix} , \text{ focusing}$$

$$\begin{bmatrix} u \\ u' \end{bmatrix} = \begin{bmatrix} 1 & 0 \\ \frac{1}{f} & 1 \end{bmatrix} \begin{bmatrix} u_0 \\ u'_0 \end{bmatrix} , \text{ defocusing.}$$



- Quadrupole doublet composed of two quadrupole magnets separated by a drift space of length L . In the thin lens approximation, if we assume that the focal length of the quadrupoles are the same, matrix becomes,

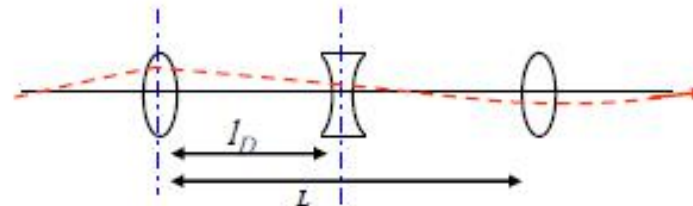
$$M = \begin{bmatrix} 1 & 0 \\ -\frac{1}{f} & 1 \end{bmatrix} \begin{bmatrix} 1 & L \\ 0 & 1 \end{bmatrix} \begin{bmatrix} 1 & 0 \\ \frac{1}{f} & 1 \end{bmatrix}$$

$$= \begin{bmatrix} 1 - \frac{L}{f} & L \\ -\frac{L}{f^2} & 1 - \frac{L}{f} \end{bmatrix}$$

Particle's transverse motion description deviating ideal orbit (x,x') by Matrix method

Transfer matrix for half a FoDo cell:

$$M_{halfCell} = \begin{pmatrix} 1 - \frac{l_D}{\tilde{f}} & l_D \\ -\frac{l_D}{\tilde{f}^2} & 1 + \frac{l_D}{\tilde{f}} \end{pmatrix}$$



Compare to the twiss parameter form of M where Φ denotes the phase advance through the half cell

$$M = \begin{pmatrix} \sqrt{\frac{\beta}{\beta_0}} (\cos \phi + \alpha \sin \phi) & \sqrt{\beta \beta_0} \sin \phi \\ \frac{(\alpha_0 - \alpha) \cos \phi - (1 + \alpha_0 \alpha) \sin \phi}{\sqrt{\beta \beta_0}} & \sqrt{\frac{\beta_0}{\beta}} (\cos \phi - \alpha \sin \phi) \end{pmatrix}$$

In the middle of a foc (defoc) quadrupole of the FoDo we always have $\alpha=0$, and the half cell will lead us from β_{max} to β_{min}

$$M = \begin{pmatrix} C & S \\ C' & S' \end{pmatrix} = \begin{pmatrix} \sqrt{\frac{\beta}{\beta_0}} \cos \phi & \sqrt{\beta \beta_0} \sin \phi \\ \frac{-1}{\sqrt{\beta \beta_0}} \sin \phi & \sqrt{\frac{\beta}{\beta_0}} \cos \phi \end{pmatrix} \quad \begin{Bmatrix} x \\ x' \end{Bmatrix} = M \begin{Bmatrix} x_0 \\ x'_0 \end{Bmatrix}$$

- Particle beam dynamics in periodic system is determined by the equation of motion (Hill's equation)

$$u'' + K(s) \cdot u = 0 \quad u \text{ represents } x \text{ or } y$$

where $K(s)$ is periodic with the period of L_p

$$K(s) = K(s + L_p)$$

Solution of the Hill's equation can be written by

$$u(s) = a\sqrt{\beta(s)} \cdot e^{\pm i\psi}$$

where $\beta(s)$ is periodic function with a period of L_p (Usually L_p is the circumference of the ring, C). ψ is called betatron phase advance and is given by

$$\psi(s - s_0) = \int_{s_0}^s \frac{d\tau}{\beta(\tau)}$$

- Phase advance per ring in the unit of 2π is called the betatron tune, ν_x and ν_y . The betatron tunes are the number of transverse oscillations per ring. We should be careful to select good values of these betatron tunes in order to avoid resonances.

Lattice or Optics Design

1.) Dipole strength: $\int B ds = N * B_0 * l_{\text{eff}} = 2\pi \frac{p}{q}$

l_{eff} effective magnet length, N number of magnets

2.) Stability condition: $|\text{Trace}(M)| < 2$

for periodic structures within the lattice / at least for the transfer matrix of the complete circular machine

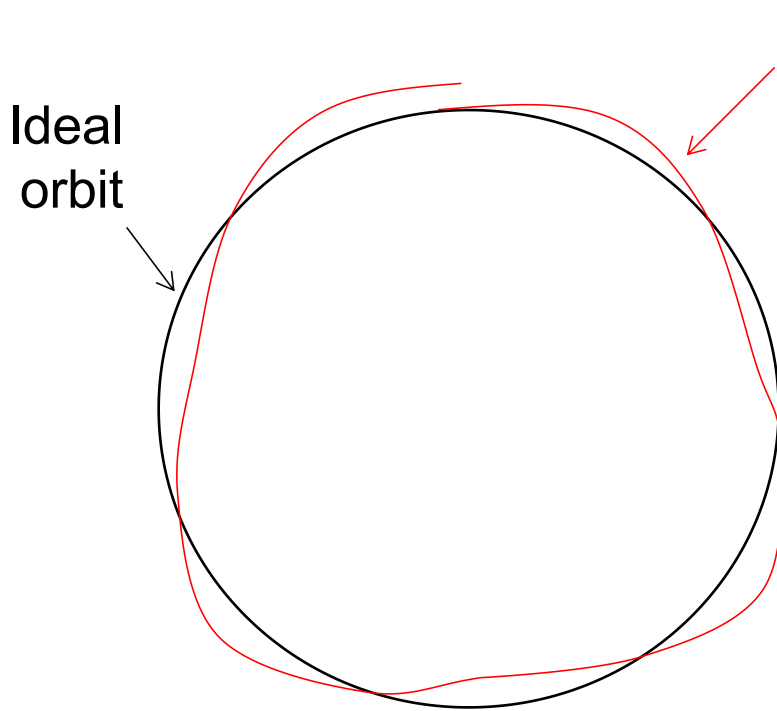
3.) Transfer matrix for periodic cell $M(s) = \begin{pmatrix} \cos \mu + \alpha(s) \sin \mu & \beta(s) \sin \mu \\ -\gamma(s) \sin \mu & \cos(\mu) - \alpha(s) \sin \mu \end{pmatrix}$

α, β, γ depend on the position s in the ring, μ (phase advance) is independent of s

4.) Thin lens approximation: $M_{QF} = \begin{pmatrix} 1 & 0 \\ \frac{1}{f_Q} & 1 \end{pmatrix} \quad f_Q = \frac{1}{k_Q l_Q}$

focal length of the quadrupole magnet $f_Q = 1/(k_Q l_Q) \gg l_Q$

Betatron Tune



Particle trajectory

- As particles go around a ring, they will undergo a number of betatrons oscillations ν (sometimes Q) given by

$$\nu = \frac{1}{2\pi} \int_s^{s+C} \frac{ds}{\beta(s)}$$

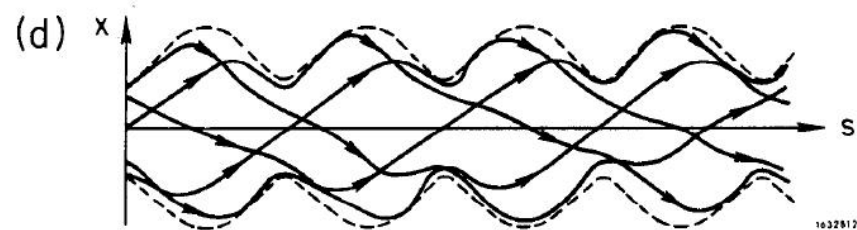
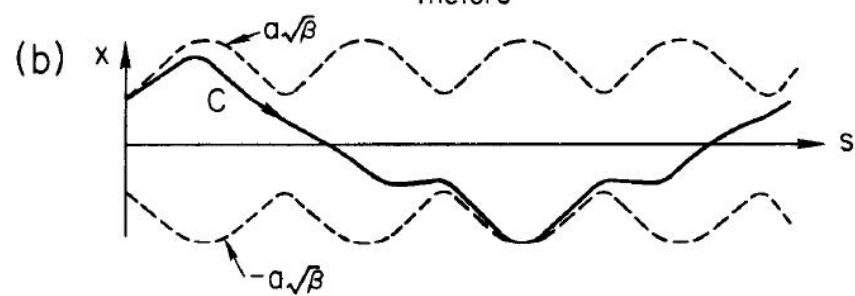
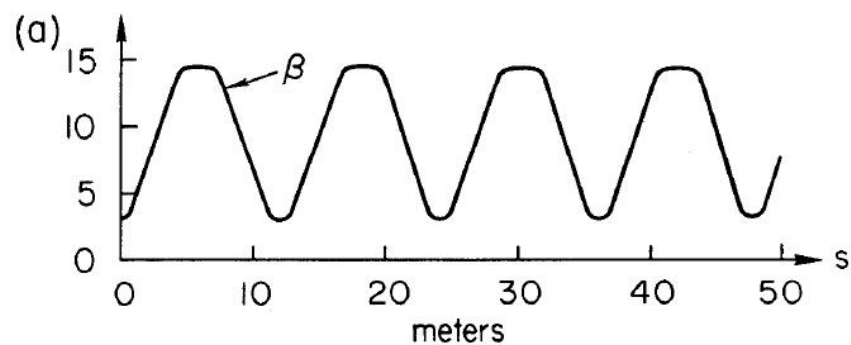
- This is referred to as the “tune”

We can generally think of the tune in two parts:

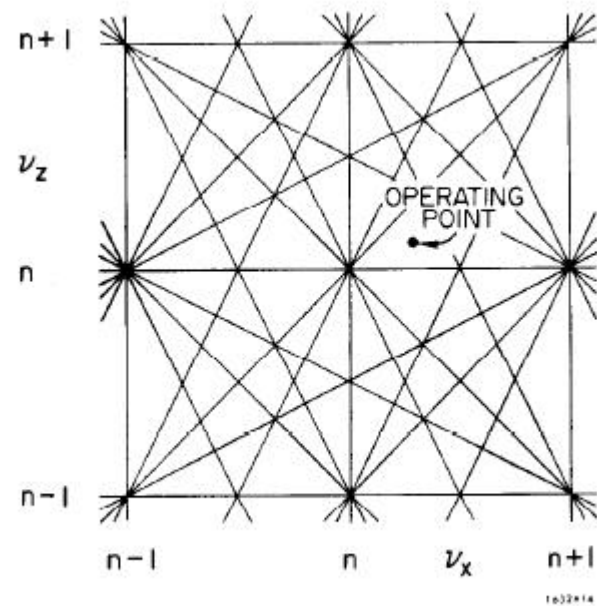
Example **6.7**

Integer : magnet/aperture optimization

Fraction: Beam Stability



1632812



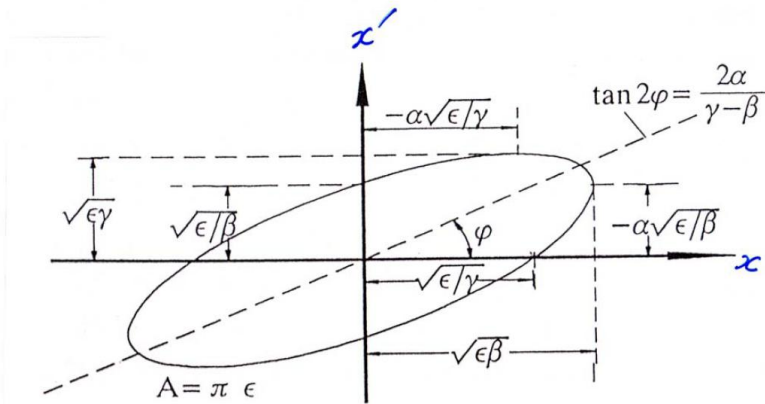
1632814

Bunch Emittance and Transverse Dimension

- If we knew the emittance we can calculate the beam size in x and y direction σ_x and σ_y from the emittance and β

$$\sigma_x = \sqrt{\varepsilon_x \beta_x}$$

$$\sigma_y = \sqrt{\varepsilon_y \beta_y}$$



- The phase space ellipse is described by

$$x^2 + 2\alpha x x' + \beta x'^2 = \varepsilon \quad ,$$

where ε is the emittance.

$$\varepsilon_x = \frac{\sigma_x^2}{\beta_x} \propto \gamma^2 \frac{\langle 1/\rho^3 \cdot H \rangle}{\langle 1/\rho^2 \rangle} \quad ,$$

where ε_x is the emittance and H is defined as:

$$H(s) = \beta \eta'^2 + 2\alpha \eta \eta' + \gamma \eta^2 \quad ,$$

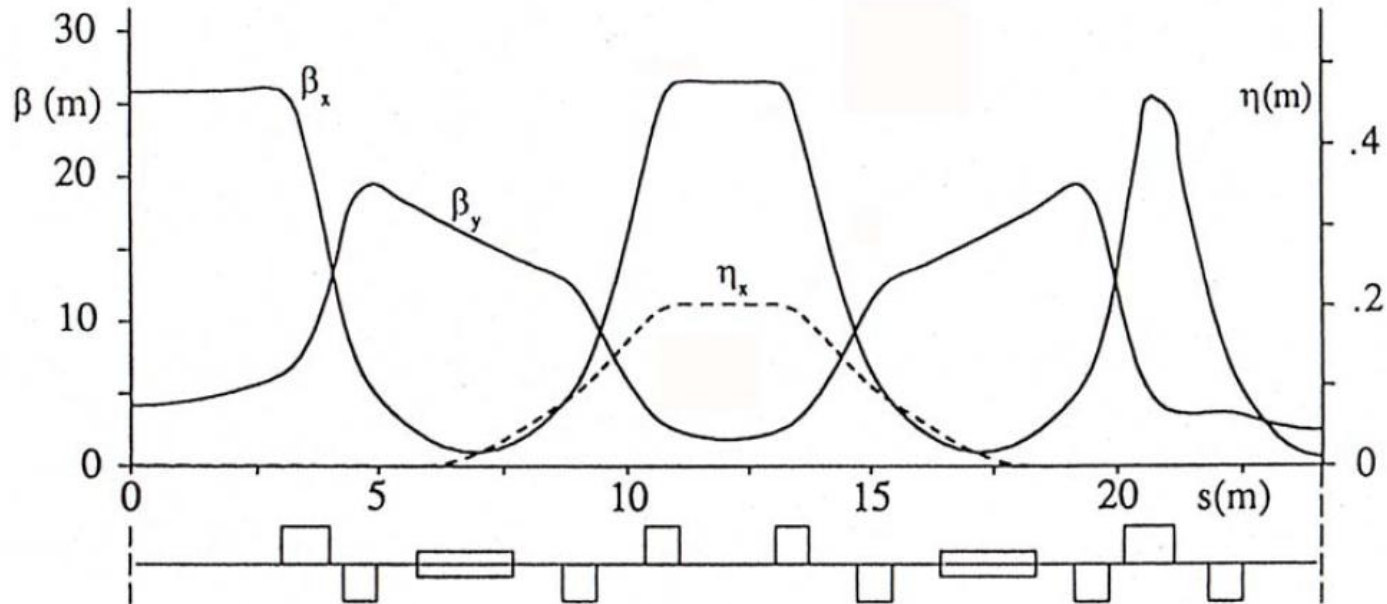
and $\langle \rangle$ means the average over the ring.

Dispersion Function

$$\mathbf{x} = \mathbf{x}_\beta + \mathbf{x}_\epsilon$$

$$\mathbf{x}_\epsilon = \eta(s) \frac{\epsilon}{E_0} \leftarrow \frac{\Delta p}{p}$$

$$\eta(s) = \frac{\sqrt{\beta(s)}}{2 \sin \pi \nu} \oint G(\bar{s}) \sqrt{\beta(\bar{s})} \cos \{ \phi(s) - \phi(\bar{s}) - \pi \nu \} d\bar{s}.$$



Momentum Compaction Factor

- Within a dipole magnet higher momentum particle has a larger radius of curvature and the lower momentum particle a smaller radius of curvature. This leads to the difference of the path length between different energy particles. The momentum compaction is defined as:

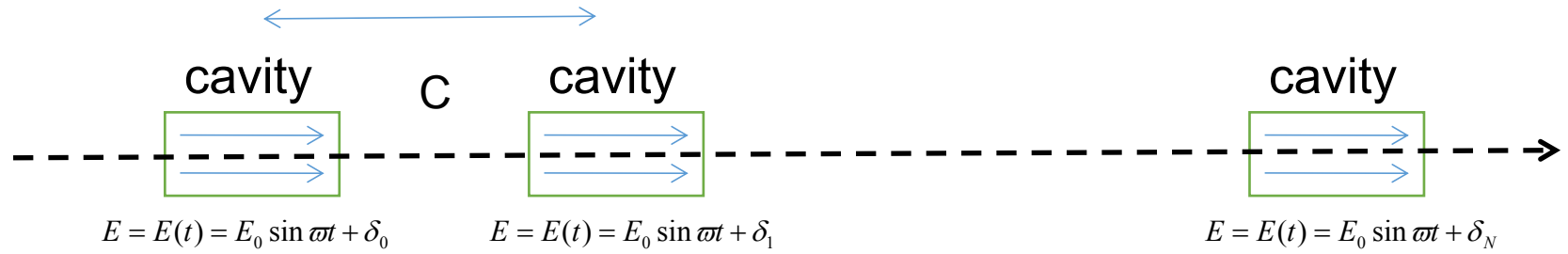
$$\alpha_c = \frac{\Delta L / L_0}{\delta}$$

α_c can be written by using the dispersion function η by

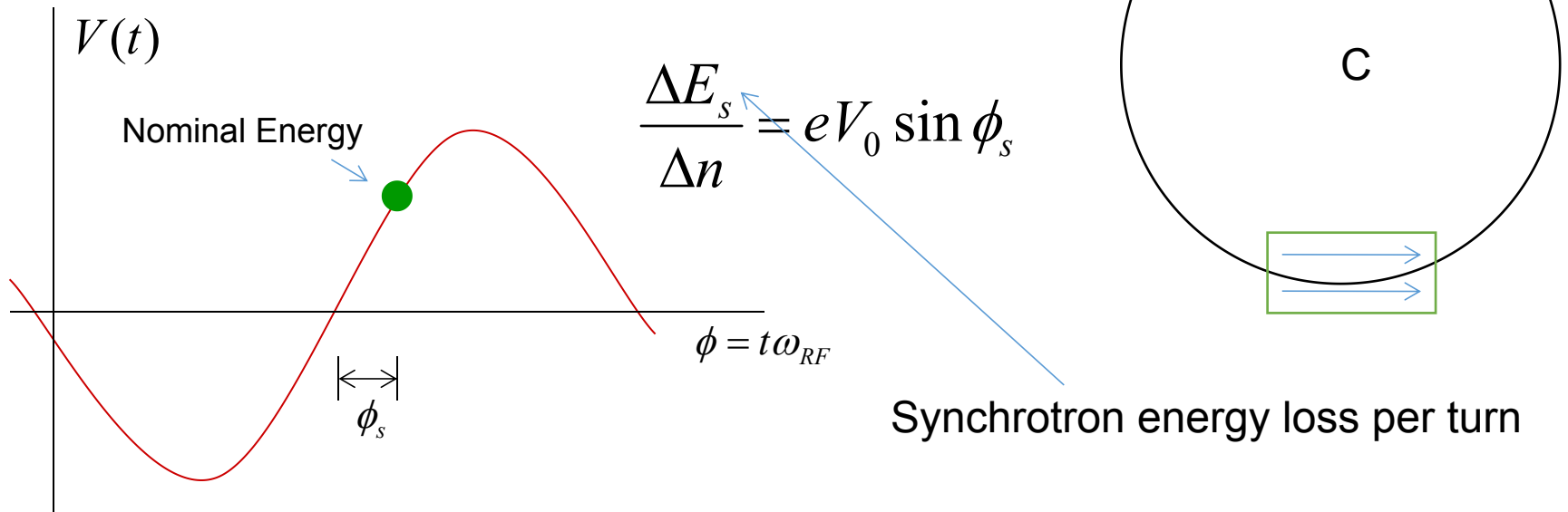
$$\alpha_c = \frac{1}{C} \oint \frac{\eta}{\rho} \cdot ds$$

Longitudinal Motion and Acceleration by RF Cavities

- We will generally accelerate particles using structures that generate time-varying electric fields (RF cavities) located within a circulating ring



we want to phase the RF so a nominal arriving particle will see the same accelerating voltage and therefore get the same boost in energy



Longitudinal Motion and Energy Oscillation

From $\frac{dE}{dt} = e\vec{v} \cdot \vec{E}$, Arrival time (minus of time of flight)

$$\Rightarrow dE = eE_z dz,$$

$$\Rightarrow \Delta E = \int eE_z dz' = eV_{RF}(-t).$$

With a proper choice of the RF cavity, we obtain

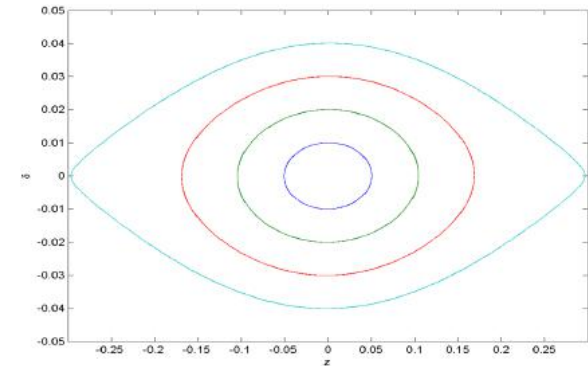
$$f_0 = c / C,$$

$$f_{RF} = hf_0,$$

$$\omega_{RF} = 2\pi f_{RF},$$

Energy gain: $E_f = E_i + eV_{RF} \sin(\omega_{RF}(-t_i) + \varphi_s).$

RF Bucket



$$\dot{\delta} = \frac{eV_{RF}k_{RF}}{\beta^2 T_0 E_0} \cos \varphi_s z$$

$$\dot{z} = -\frac{\eta C}{T_0} \delta$$

Synchrotron tune is given by

$$\nu_s = \sqrt{\frac{h\eta}{2\pi} \frac{eV_{RF}}{\beta^2 E_0} \cos \varphi_s},$$

where $\omega_s = \nu_s \omega_0$.

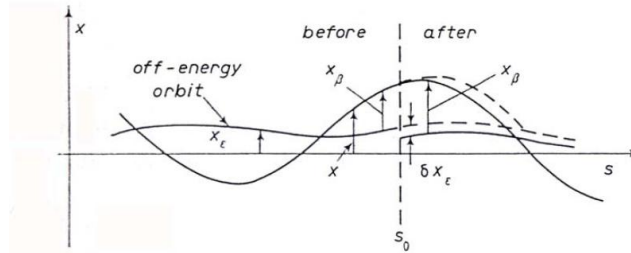
Synchrotron Radiation: Quantum Excitation and Radiation Damping

- SR is quantum emission. When a quantum of energy u is emitted, the energy of the electron is suddenly decreased by the amount of u . This impulsive disturbances – occurring at random times – causes the energy oscillation to grow. This growth is limited – on the average – by the damping. This mechanism determines the energy spread σ_ε :

$$\sigma_\varepsilon \approx \sqrt{E_0 u_c}$$

- Bunch length is proportional to the energy spread:

$$\sigma_\tau = \frac{\alpha_c}{\Omega E_0} \sigma_\varepsilon$$



Effect of a sudden energy change at s_0 on the betatron displacement.

- The emission of discrete quanta in SR will also excite random betatron oscillations, and these quantum-induced oscillations are responsible for the lateral extent of a stored electron beam.
- The emission of a quantum of energy u will result in a change δx_b in the betatron displacement and a change $\delta x'_b$ in the betatron slope given by,

$$\delta x_\beta = -\eta \frac{u}{E_0}$$

$$\delta x'_\beta = -\eta' \frac{u}{E_0}$$

- In the vertical direction, if the machine is perfectly made, there is no dispersion. This means that in an ideal case the beam size in the vertical direction should be zero. In reality, however, due to imperfections of the machine such as misalignment, etc., there appears a small residual dispersion in the vertical direction. This causes a finite vertical beam size in the vertical direction. Usually the ratio of the vertical emittance to the horizontal emittance is of the order of a few percent.

Multi-Particle (collective) and Non-Linear Dynamics in Storage Ring and Colliders

Luminosity from Physics

The relationship of the beam to the rate of observed physics processes is given by the “Luminosity”

$$\text{Rate} \rightarrow R = L\sigma$$

“Luminosity” \swarrow L \nwarrow Cross-section (“physics”) σ

Standard unit for Luminosity is $\text{cm}^{-2}\text{s}^{-1}$

Standard unit of cross section is “barn”= 10^{-24} cm^2

Integrated luminosity is usually in barn^{-1} , where $\text{b}^{-1} = (1 \text{ sec}) \times (10^{24} \text{ cm}^{-2}\text{s}^{-1})$

$\text{nb}^{-1} = 10^9 \text{ b}^{-1}$, $\text{fb}^{-1} = 10^{15} \text{ b}^{-1}$, etc

For (thin) fixed target:

$$R = N\rho_n t\sigma \Rightarrow L = N\rho_n t$$

Incident rate \nearrow R \nearrow N \nearrow ρ_n \nearrow t Target thickness

Target number density

Luminosity from Colliding Beams

- For equally intense Gaussian beams

Collision frequency

Particles in a bunch

$$L = f \frac{N_b^2}{4\pi\sigma^2} R$$

Geometrical factor:

- crossing angle
- hourglass effect
- crab waist

Transverse size
(RMS)

- Expressing this in terms of our usual beam parameters

$$L = f_{rev} \frac{1}{4\pi} n N_b^2 \frac{\gamma}{\beta^* \varepsilon_N} R$$

Revolution frequency

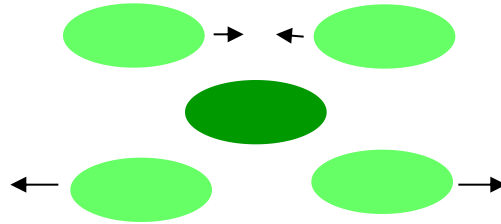
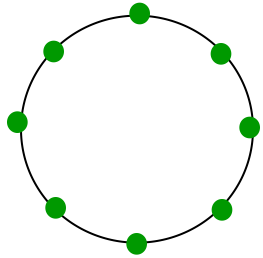
Number of bunches

Normalized emittance

Betatron function at
collision point

Luminosity from Colliding Beams

Circulating beams typically “bunched”



(number of interactions)

$$= \left(\frac{N_1}{A} \right) N_2 \sigma$$

Cross-sectional
area of beam

Total Luminosity:

$$L = \left(\frac{N_1 N_2}{A} \right) r_b = \left(\frac{N_1 N_2}{A} \right) n \frac{c}{C}$$

Number of
bunches

Circumference
of machine

Record e⁺e⁻ Luminosity (KEK-B):

2.11x10³⁴ cm⁻²s⁻¹

Record p-p̄ Luminosity (Tevatron):

4.06x10³² cm⁻²s⁻¹

Record Hadronic Luminosity (LHC):

3.60x10³³ cm⁻²s⁻¹

LHC Design Luminosity:

1.00x10³⁴ cm⁻²s⁻¹

CEPC

3.00x10³⁴ cm⁻²s⁻¹

Luminosity from Colliding Beams

- For equally intense Gaussian beams

$$L = f \frac{N_b^2}{4\pi\sigma_x\sigma_y} R$$

Collision frequency

Particles in a bunch

Geometrical factor:
- crossing angle
- hourglass effect

Transverse beam size (RMS)

- Expressing luminosity in terms of our usual beam parameters

$$L[\text{cm}^{-2}\text{s}^{-1}] = 2.17 \times 10^{34} (1+r) \xi_y \frac{E[\text{GeV}] I[\text{A}]}{\beta_y[\text{cm}]}$$

where

$$\xi_y = \frac{r_e N_e \beta_y}{2\pi\sigma_y(\sigma_x + \sigma_y)} :$$

Maximum Beam-beam Tune Shift Analytical Expressions for Lepton and Hadron Circular Colliders

For lepton collider:

$$\xi_{y, \max} = \frac{2845}{2\pi} \sqrt{\frac{T_0}{\tau_y \gamma N_{IP}}} \quad \xi_{y, \max} = \frac{2845\gamma}{1} \sqrt{\frac{r_e}{6\pi R N_{IP}}}$$

r_e is electron radius
 γ is normalized energy
 R is the dipole bending radius
 N_{IP} is number of interaction points

$$\xi_{x, \max} = \sqrt{2} \xi_{y, \max}$$

J. Gao, Nuclear Instruments and Methods in Physics Research A 533 (2004) 270–274

J. Gao, Nuclear Instruments and Methods in Physics Research A 463 (2001) 50–61

For hadron collider:

$$\xi_{\max} = \frac{2845\gamma}{f(x)} \sqrt{\frac{r_p}{6\pi R N_{IP}}}$$

where r_p is proton radius

$$f(x) = 1 - \frac{2}{\sqrt{2\pi}} \int_0^x \exp\left(-\frac{t^2}{2}\right) dt$$

$$X^2 = \frac{4f(x)}{\pi \xi_{\max} N_{IP}} = \frac{4f^2(x)}{2845\pi\gamma} \sqrt{\frac{6\pi R}{r_p N_{IP}}}$$

J. Gao, "Review of some important beam physics issues in electron positron collider designs",
Modern Physics Letters A, Vol. 30, No. 11 (2015)
1530006 (20 pages)

J. Gao, et al, "Analytical estimation of maximum beam-beam tune shifts for electron-positron and hadron circular colliders", Proceedings of ICFA Workshop on High Luminosity Circular e+e- Colliders – Higgs Factory, 2014

Analytical Treatment of Dynamic Apertures of Multipoles

$$\begin{aligned}
 \Psi &= \int_0^s \frac{ds'}{\beta_x(s')} + \phi_0 \\
 J &= \frac{\varepsilon_x}{2} = \frac{1}{2\beta_x(s)} \left(x^2 + \left(\beta_x(s)x' - \frac{\beta'_x x}{2} \right)^2 \right) \Rightarrow \\
 H(J, \Psi) &= \frac{J}{\beta_x(s)} \\
 x &= \sqrt{2J_1 \beta_x(s)} \cos \left(\Psi_1 - \frac{2\pi\nu}{L}s + \int_0^s \frac{ds'}{\beta_x(s')} \right) \\
 \Psi_1 &= \Psi + \frac{2\pi\nu}{L} - \int_0^s \frac{ds'}{\beta_x(s')} \\
 J_1 &= J \\
 H_1 &= \frac{2\pi\nu}{L} J_1 \\
 \frac{dJ_1}{ds} &= -\frac{\partial H_1}{\partial \Psi_1} \\
 \frac{d\Psi_1}{ds} &= \frac{\partial H_1}{\partial J_1} \Rightarrow \\
 \overline{J_1} &= \overline{J_1}(\Psi_1, J_1) \\
 \overline{\Psi_1} &= \overline{\Psi_1}(\Psi_1, J_1) \\
 \overline{I} &= I + K_0 \sin \theta \\
 \overline{\theta} &= \theta + \overline{I} \Rightarrow |K_0| \leq 1 \quad (0.97164) \Rightarrow \text{Analytical DA expressions}
 \end{aligned}$$

$$\begin{aligned}
 I &= \frac{x^2 B_y|_{x=0,y=0}}{2\rho^2 B_0} \\
 &+ \frac{1}{B_0 \rho} \sum_{n=1}^{\infty} \frac{1}{n!} \frac{\partial^{n-1} B_y}{\partial x^{n-1}} \Big|_{x=0,y=0} (x + iy)^n \\
 &- (1 + x/\rho) \left(1 + \frac{\Delta P}{P_0} - \left(\bar{p}_x - \frac{eA_x}{P_0} \right)^2 \right. \\
 &\left. - \left(\bar{p}_y - \frac{eA_y}{P_0} \right)^2 \right)^{1/2} - \frac{e\Phi}{P_0}
 \end{aligned}$$

J. Gao, "Analytical estimation of the dynamic apertures of circular accelerators", **Nuclear Instruments and Methods in Physics Research A** 451 (2000) 545-557.

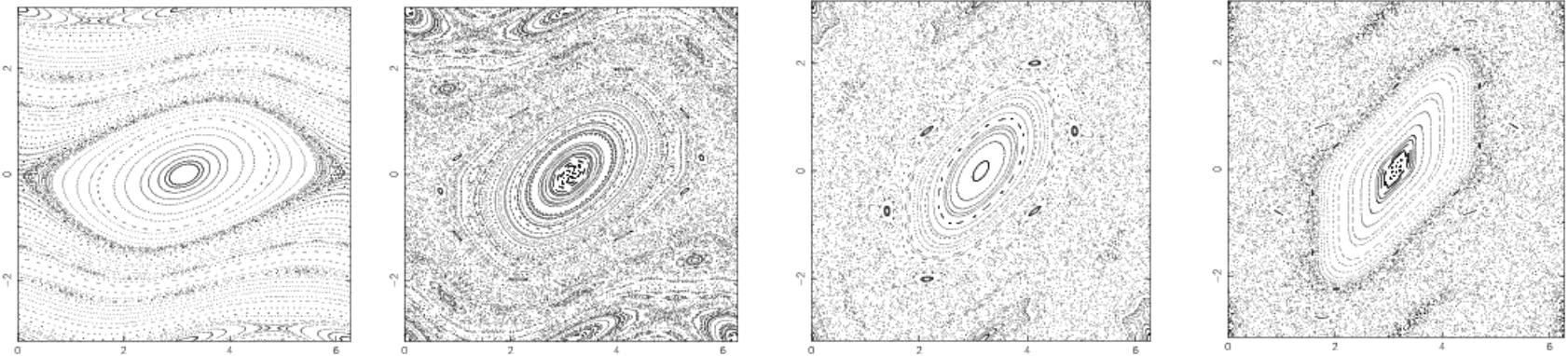
Standard Map

The progresses of nonlinear physics are the bases for understanding various long stadind beam dynamics phenomenons.

$$\bar{I} = I + K_0 \sin \theta$$

$$\bar{\theta} = \theta + \bar{I}$$

when $K \geq 0.97164$ stochastic motion starts,
so called Chirikov Criterion



Chirikov, B. V. "A Universal Instability of Many-Dimensional Oscillator Systems." **Phys. Rep.** 52, 264-379, 1979.

*R.Z. Sagdeev, D.A. Usikov, G.M. Zaslavsky, **Nonlinear Physics, from the Pendulum to Turbulence and Chaos**, Harwood Academic Publishers, 1988.

Basic Theory of Dynamic Aperture

$$H = \frac{p^2}{2} + \frac{K(s)}{2} x^2 + \frac{1}{m! B_0 \rho} \frac{\partial^{m-1} B_z}{\partial x^{m-1}} x^m L \sum_{k=-\infty}^{\infty} \delta(s-kL)$$

$$B_z = B_0(1 + x b_1 + x^2 b_2 + x^3 b_3 + \dots + x^{m-1} b_{m-1} + \dots)$$

For one multipole $B_z = B_0 x^{m-1} b_{m-1}$ $m \geq 3$

$$A_{\text{dyna}, 2m} = \sqrt{2\beta_x(s)} \left(\frac{1}{m\beta_x^m(s(2m))} \right)^{\frac{1}{2(m-2)}} \left(\frac{\rho}{|b_{m-1}|L} \right)^{1/(m-2)}$$

Relation between X and Y $A_{\text{dyna}, 2m, y} = \sqrt{\frac{\beta_x(s(2m))}{\beta_y(s(2m))} (A_{\text{dyna}, 2m, x}^2 - x^2)}$

For more independent
multipoles

$$A_{\text{dyna}, \text{total}} = \frac{1}{\sqrt{\sum_i \frac{1}{A_{\text{dyna}, \text{sext}, i}^2} + \sum_j \frac{1}{A_{\text{dyna}, \text{oct}, j}^2} + \sum_k \frac{1}{A_{\text{dyna}, \text{deca}, k}^2} + \dots}}$$

Circular machine

A nonlinear
multipole

Standard Mapping
Chirikov Criterion

Hénon and
Heiles problem

Circular machine

Many multipoles

J. Gao, "Analytical estimation of the dynamic apertures of circular accelerators", **Nuclear Instruments and Methods in Physics Research A** 451 (2000) 545-557.

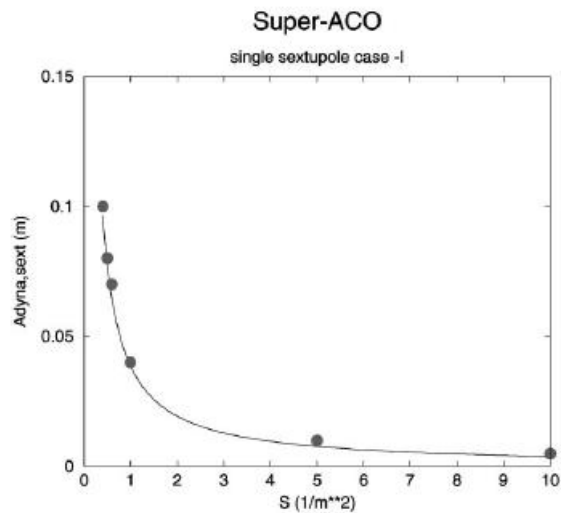


Fig. 16. The dynamic aperture of Super-ACO vs S ($S = b_2 L / \rho$) at s_1 .

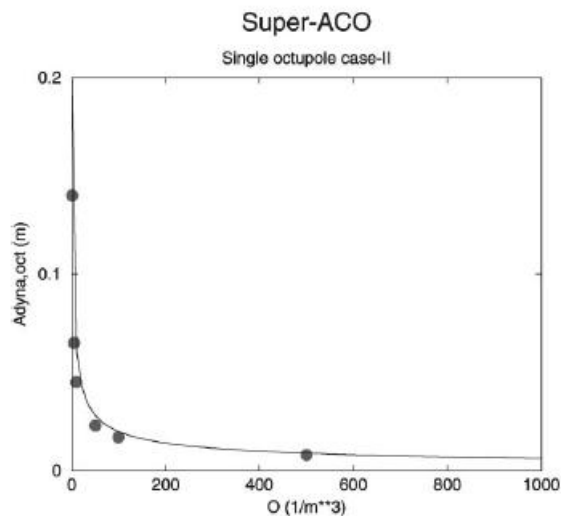


Fig. 17. The dynamic aperture of Super-ACO vs O ($O = b_3 L / \rho$) at s_2 .

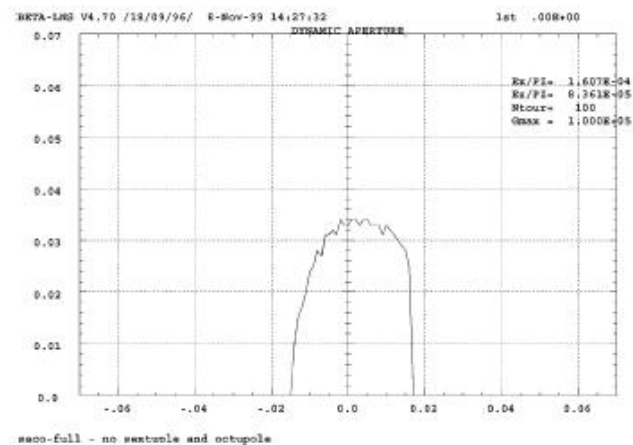


Fig. 22. The 2D dynamic aperture of Super-ACO with $S = 2$ located at s_2 with $\beta_x(s_2) = 15.18$ m and $\beta_y(s_2) = 4.26$ m.

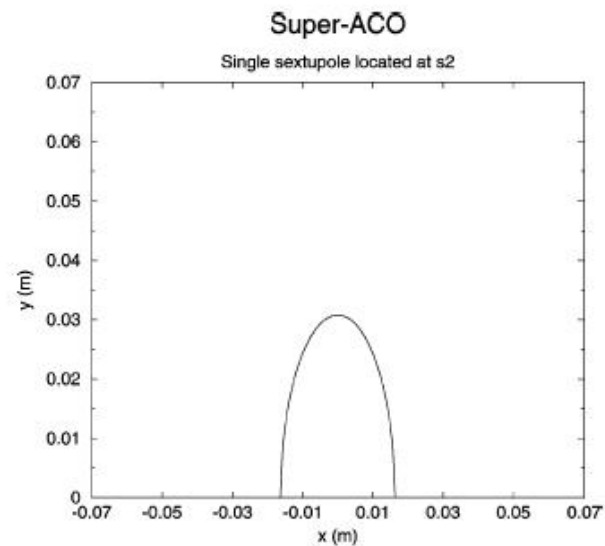


Fig. 23. The analytical estimation of the 2D dynamic aperture of Super-ACO with $S = 2$ located at s_2 with $\beta_x(s_2) = 15.8$ m and $\beta_y(s_2) = 4.26$ m.

Super-ACO

Table 1
Summary of parameters

Case	Multipole strength	Beta function (m)
1	$S(s_1) = 2 \text{ (1/m}^2\text{)}$	$\beta_x(s_1) = 13.6$
2	$O(s_1) = 10 \text{ (1/m}^3\text{)}$	$\beta_x(s_1) = 13.6$
3	$D(s_1) = 1000 \text{ (1/m}^4\text{)}$	$\beta_x(s_1) = 13.6$
4	$S(s_1) = 2 \text{ (1/m}^2\text{)},$ $O(s_1) = 62 \text{ (1/m}^3\text{)}$	$\beta_x(s_1) = 13.6$
5	$S(s_1) = 2 \text{ (1/m}^2\text{)},$ $O(s_2) = 62 \text{ (1/m}^3\text{)}$	$\beta_x(s_1) = 13.6,$ $\beta(s_2) = 15.18$
6	$S(s_{1,2,3,4}) = 2 \text{ (1/m}^2\text{)}$	$\beta_x(s_{1,2,3,4}) = 13.6,$ 15.18, 7.8, 6.8
8	$S(s_1) = 2 \text{ (1/m}^2\text{)}$	$\beta_x(s_1) = 12.42, \beta_x(0) = 5.1$
9	$S(s_1) = 2 \text{ (1/m}^2\text{)}$	$\beta_x(s_2) = 15.18$

Table 2
Summary of comparison results

Case	$A_{\text{dyna,analy.}} \text{ (m)}$	$A_{\text{dyna,numer.}} \text{ (m)}$
1	0.0385	0.04
2	0.055	0.054
3	0.022	0.024
4	0.0145	0.016
5	0.0138	0.0135
6	0.012	0.0135
8	0.021	0.02
9	$A_x = 0.0163,$ $A_y = 0.031$	$A_x = 0.017,$ $A_y = 0.034$

Dynamic Aperture of Wigglers

A example of a sum of multipoles

$$B_x = \frac{k_x}{k_y} B_0 \sinh(k_x x) \sinh(k_y y) \cos(ks), \quad (1)$$

$$B_y = B_0 \cosh(k_x x) \cosh(k_y y) \cos(ks), \quad (2)$$

$$B_z = -\frac{k}{k_y} B_0 \cosh(k_x x) \sinh(k_y y) \sin(ks) \quad (3)$$

$$A_{N_w, y}(s) = \sqrt{\frac{3\beta(s)}{\beta_{y,m}^2} \frac{\rho_w}{k_y \sqrt{L_w}}},$$

$$A_{N_w, x}(s) = \sqrt{\frac{\beta_y(s)}{\beta_x(s)} (A_{N_w, y}(s)^2 - y^2)}.$$

Wiggler fields

$$A_{\text{total}, y}(s) = \frac{1}{\sqrt{1/A_y(s)^2 + \sum_{j=1}^M 1/A_{j, w, y}(s)^2}},$$

where N_w is the wiggler period number, λ_w is the wiggler period length, the wiggler length $L_w = N_w \lambda_w$, ρ_w is the radius of curvature of the wiggler peak magnetic field B_0 , and $\rho_w = E_0/ecB_0$ with E_0 being the electron energy, and $\beta_{y,m}$ is the beta function value in the middle of the wiggler.

J. Gao, “Analytical estimation of dynamic apertures limited by the wigglers in storage rings”, **Nuclear Instruments and Methods in Physics Research A** 516 (2004) 243–248

Super-ACO

Table 1

The dynamic apertures correspond to different ρ_w , where $A_{N_w,y,n}$ and $A_{N_w,y,a}$ correspond to numerical and analytical results, respectively

ρ_w (m)	$A_{N_w,y,n}$ (m)	$A_{N_w,y,a}$ (m)	$\beta_{y,m}$ (m)	λ_w (m)	L_w (m)
2.7	0.017	0.019	13	0.17584	3.5168
3	0.023	0.024	10.7	0.17584	3.5168
4	0.033	0.034	9.5	0.17584	3.5168

Table 2

The dynamic apertures correspond to different λ_w , where $A_{N_w,y,n}$ and $A_{N_w,y,a}$ correspond to numerical and analytical results, respectively

λ_w (m)	$A_{N_w,y,n}$ (m)	$A_{N_w,y,a}$ (m)	$\beta_{y,m}$ (m)	ρ_w (m)	L_w (m)
0.08792	0.016	0.017	9.55	4	3.5168
0.17584	0.033	0.034	9.5	4	3.5168
0.35168	0.067	0.067	9.5	4	3.5168

One wiggler
case

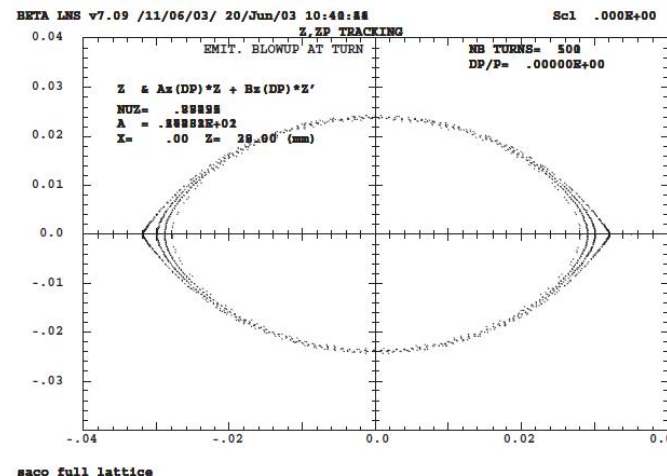


Fig. 5. The vertical phase space corresponds to the case of two wigglers.

When $\rho_w = 6$ m and $\beta_y(s) = \beta_{y,m} = 13.75$ m, one finds the vertical dynamic aperture limited by the two wigglers being 0.032 m numerically as shown in Fig. 5 and 0.03 m analytically calculated from Eqs. (19) and (23).

Two wiggler case

Nonlinear Beam-Beam Effects-1 (e+e-)

Bsseti-Erskine formula for beam-beam induced transverse kicks

$$\delta y' + i\delta x' = -\frac{N_e r_e}{\gamma_*} f(x, y, \sigma_x, \sigma_y)$$

$$f(x, y, \sigma_x, \sigma_y) = \sqrt{\frac{2\pi}{\sigma_x^2 - \sigma_y^2}} \times w\left(\frac{x + iy}{\sqrt{2(\sigma_x^2 - \sigma_y^2)}}\right) - \sqrt{\frac{2\pi}{\sigma_x^2 - \sigma_y^2}} \times \exp\left(-\frac{x^2}{2\sigma_x^2} - \frac{y^2}{2\sigma_y^2}\right) w\left(\frac{\frac{\sigma_y}{\sigma_x}x + i\frac{\sigma_x}{\sigma_y}y}{\sqrt{2(\sigma_x^2 - \sigma_y^2)}}\right)$$

$$H_y = \frac{p_y^2}{2} + \frac{K_y(s)}{2} y^2 + \frac{N_e r_e}{\sqrt{2}\gamma_*} \left(\frac{1}{\sigma_x \sigma_y} y^2 - \frac{1}{12\sigma_x \sigma_y^3} y^4 + \frac{1}{120\sigma_x \sigma_y^5} y^6 - \frac{1}{1344\sigma_x \sigma_y^7} y^8 + \dots \right) \times \sum_{k=-\infty}^{\infty} \delta(s - kL) \quad (\text{FB}), \quad (38)$$

with $p_x = dx/ds$ and $p_y = dy/ds$.

J. Gao, “Analytical estimation of the beam–beam interaction limited dynamic apertures and lifetimes in e+e- circular colliders”, **Nuclear Instruments and Methods in Physics Research A** 463 (2001) 50–61

Nonlinear Beam-Beam Effects-2 (e+e-)

$$\tau_{bb} = \frac{\tau_y}{2} \left(\frac{\langle y^2 \rangle}{y_{\max}^2} \right) \exp \left(\frac{y_{\max}^2}{\langle y^2 \rangle} \right) = \frac{\tau_y}{2} \left(\frac{\sigma_y(s)^2}{A_{\text{dyna},y}(s)^2} \right) \exp \left(\frac{A_{\text{dyna},y}(s)^2}{\sigma_y(s)^2} \right)$$

or

$$\tau_{bb,y}^* = \frac{\tau_y^*}{2} \left(\frac{16\gamma_* \sigma^2}{N_e r_e \beta_y(s_{\text{IP}})} \right)^{-1} \exp \left(\frac{16\gamma_* \sigma^2}{N_e r_e \beta_y(s_{\text{IP}})} \right) \quad (\text{RB})$$

$$\tau_{bb,y}^* = \frac{\tau_y^*}{2} \left(\frac{4}{\pi \xi_y^*} \right)^{-1} \exp \left(\frac{4}{\pi \xi_y^*} \right) \quad (\text{RB})$$

$$\tau_{bb,x}^* = \frac{\tau_x^*}{2} \left(\frac{6\gamma_* \sigma_x^2}{N_e r_e \beta_x(s_{\text{IP}})} \right)^{-1} \exp \left(\frac{6\gamma_* \sigma_x^2}{N_e r_e \beta_x(s_{\text{IP}})} \right) \quad (\text{FB})$$

$$\tau_{bb,x}^* = \frac{\tau_x^*}{2} \left(\frac{3}{\pi \xi_x^*} \right)^{-1} \exp \left(\frac{3}{\pi \xi_x^*} \right) \quad (\text{FB})$$

$$\tau_{bb,y}^* = \frac{\tau_y^*}{2} \left(\frac{3\sqrt{2}\gamma_* \sigma_x \sigma_y}{N_e r_e \beta_y(s_{\text{IP}})} \right)^{-1} \exp \left(\frac{3\sqrt{2}\gamma_* \sigma_x \sigma_y}{N_e r_e \beta_y(s_{\text{IP}})} \right) \quad (\text{FB})$$

$$\tau_{bb,y}^* = \frac{\tau_y^*}{2} \left(\frac{3}{\sqrt{2}\pi \xi_y^*} \right)^{-1} \exp \left(\frac{3}{\sqrt{2}\pi \xi_y^*} \right) \quad (\text{FB}).$$

More generally, one has

$$\tau_{bb,2m,y}^* = \frac{\tau_y^*}{2} \left(\frac{2^{(m-2)/2} C_{m,\text{RB}}}{4\pi \sqrt{m} \xi_y^*} \right)^{-2/m-2} \exp \left(\left(\frac{2^{(m-2)/2} C_{m,\text{RB}}}{4\pi \sqrt{m} \xi_y^*} \right)^{2/m-2} \right) \quad (\text{RB})$$

$$\tau_{bb,2m,x}^* = \frac{\tau_x^*}{2} \left(\frac{2^{(m-2)/2} C_{m,\text{FB},x}}{\pi 2 \sqrt{m} \xi_x^*} \right)^{-2/m-2} \exp \left(\left(\frac{2^{(m-2)/2} C_{m,\text{FB},x}}{\pi 2 \sqrt{m} \xi_x^*} \right)^{2/m-2} \right) \quad (\text{FB})$$

Nonlinear Beam-Beam Effects-3 (e+e-)

$$\xi_x^* = \frac{N_e r_e \beta_{x,IP}}{2\pi\gamma^* \sigma_x (\sigma_x + \sigma_y)}$$

$$\xi_y^* = \frac{N_e r_e \beta_{y,IP}}{2\pi\gamma^* \sigma_y (\sigma_x + \sigma_y)}$$

Dynamic apertures limited by nonlinear beam-beam effects

$$\frac{A_{\text{dyna},8,y}(s)}{\sigma_{*,y}(s)} = \left(\frac{16\gamma_* \sigma^2}{N_e r_e \beta_y(s_{IP})} \right)^{1/2} \quad (\text{RB}) \quad = \left(\frac{4}{\pi \xi_y^*} \right)^{1/2}$$

$$\frac{A_{\text{dyna},8,x}(s)}{\sigma_{*,x}(s)} = \left(\frac{6\gamma_* \sigma_x^2}{N_e r_e \beta_x(s_{IP})} \right)^{1/2} \quad (\text{FB}) \quad = \left(\frac{3}{\pi \xi_x^*} \right)^{1/2}$$

$$\frac{A_{\text{dyna},8,y}(s)}{\sigma_{*,y}(s)} = \left(\frac{3\sqrt{2}\gamma_* \sigma_x \sigma_y}{N_e r_e \beta_y(s_{IP})} \right)^{1/2} \quad (\text{FB}). \quad = \left(\frac{3}{\sqrt{2}\pi \xi_y^*} \right)^{1/2}$$

Nonlinear Beam-Beam Effects-4 (e+e-)

More generally, one has

$$\tau_{bb,2m,y}^* = \frac{\tau_y^*}{2} \left(\frac{2^{(m-2)/2} C_{m, \text{RB}}}{4\pi\sqrt{m}\xi_y^*} \right)^{-2/m-2} \exp \left(\left(\frac{2^{(m-2)/2} C_{m, \text{RB}}}{4\pi\sqrt{m}\xi_y^*} \right)^{2/m-2} \right) \quad (\text{RB})$$

$$\tau_{bb,2m,x}^* = \frac{\tau_x^*}{2} \left(\frac{2^{(m-2)/2} C_{m, \text{FB},x}}{\pi 2\sqrt{m}\xi_x^*} \right)^{-2/m-2} \exp \left(\left(\frac{2^{(m-2)/2} C_{m, \text{FB},x}}{\pi 2\sqrt{m}\xi_x^*} \right)^{2/m-2} \right) \quad (\text{FB})$$

$$\tau_{bb,2m,y}^* = \frac{\tau_y^*}{2} \left(\frac{2^{(m-2)/2} C_{m, \text{FB},y}}{\pi\sqrt{2m}\xi_y^*} \right)^{-2/m-2} \exp \left(\left(\frac{2^{(m-2)/2} C_{m, \text{FB},y}}{\pi\sqrt{2m}\xi_y^*} \right)^{2/m-2} \right) \quad (\text{FB}).$$

$$\xi_{y,\text{max}}^{\text{RB}} = \frac{4\sqrt{2}}{3} \xi_{y,\text{max}}^{\text{FB}} = 1.89 \xi_{y,\text{max}}^{\text{FB}}$$

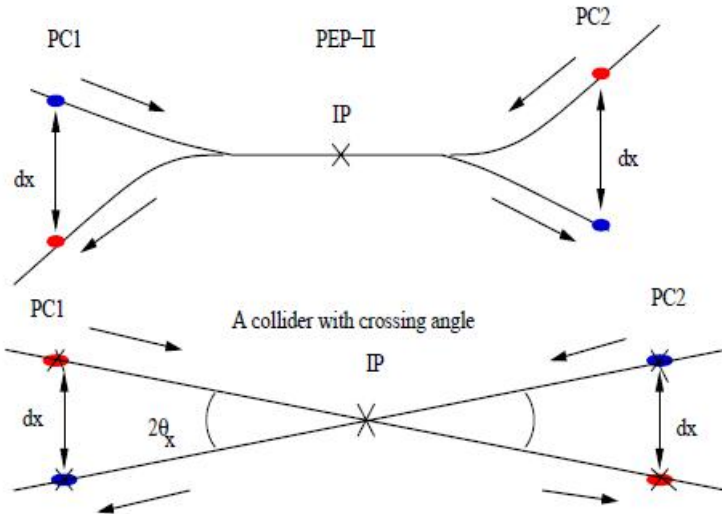
Round beam vs flat beam

and

$$\xi_{x,\text{max}}^{\text{FB}} = \sqrt{2} \xi_{y,\text{max}}^{\text{FB}}.$$

J. Gao, “Analytical estimation of the beam–beam interaction limited dynamic apertures and lifetimes in e+e- circular colliders”, **Nuclear Instruments and Methods in Physics Research A** 463 (2001) 50–61

Parasitic Crossing Beam-Beam Effects



with

$$\tau_{PC,y,RB} = \frac{\tau_y}{2} (\mathcal{R}_{y,PC,RB})^{-1} \exp(\mathcal{R}_{y,PC,RB})$$

$$= \frac{\tau_y}{2} \left(\frac{4}{\pi \xi_{PC,y}} \right)^{-1} \exp \left(\frac{4}{\pi \xi_{PC,y}} \right)$$

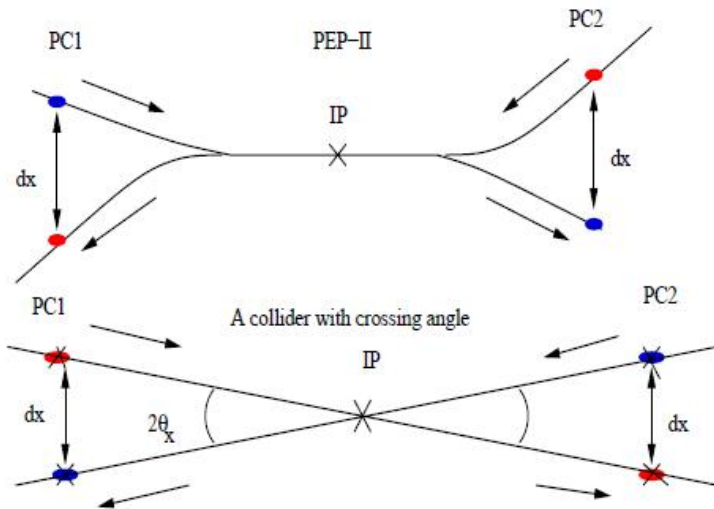
$$\xi_{PC,y} = \frac{r_e N_e \beta_{PC,x}}{2\pi \gamma_* \Sigma_{PC}^2} = \frac{r_e N_e \beta_{PC,y}}{2\pi \gamma_* d_x^2}$$

$$\Sigma_{PC}, \Sigma_{PC} = \sqrt{d_x^2 + d_y^2}$$

J. Gao, ON PARASITIC CROSSINGS AND THEIR LIMITATIONS TO E+E- STORAGE RING COLLIDERS, **Proceedings of EPAC 2004**, Lucerne, Switzerland, p. 671-673 (2004)

J. Gao, "Analytical treatment of the nonlinear electron cloud effect and the combined effects with beam-beam and space charge nonlinear forces in storage rings", **Chinese Physics C** Vol. 33, No. 2, Feb., 2009, 135-144

Beam-Beam Effects with Crossing Angle



$$\mathcal{R}_{\text{syn-beta},x} = \frac{A_{\text{syn-beta},x}(s)^2}{\sigma_x(s)^2} = \frac{2}{3\pi^2} \left(\frac{1}{\xi_x^* \Phi} \right)^2$$

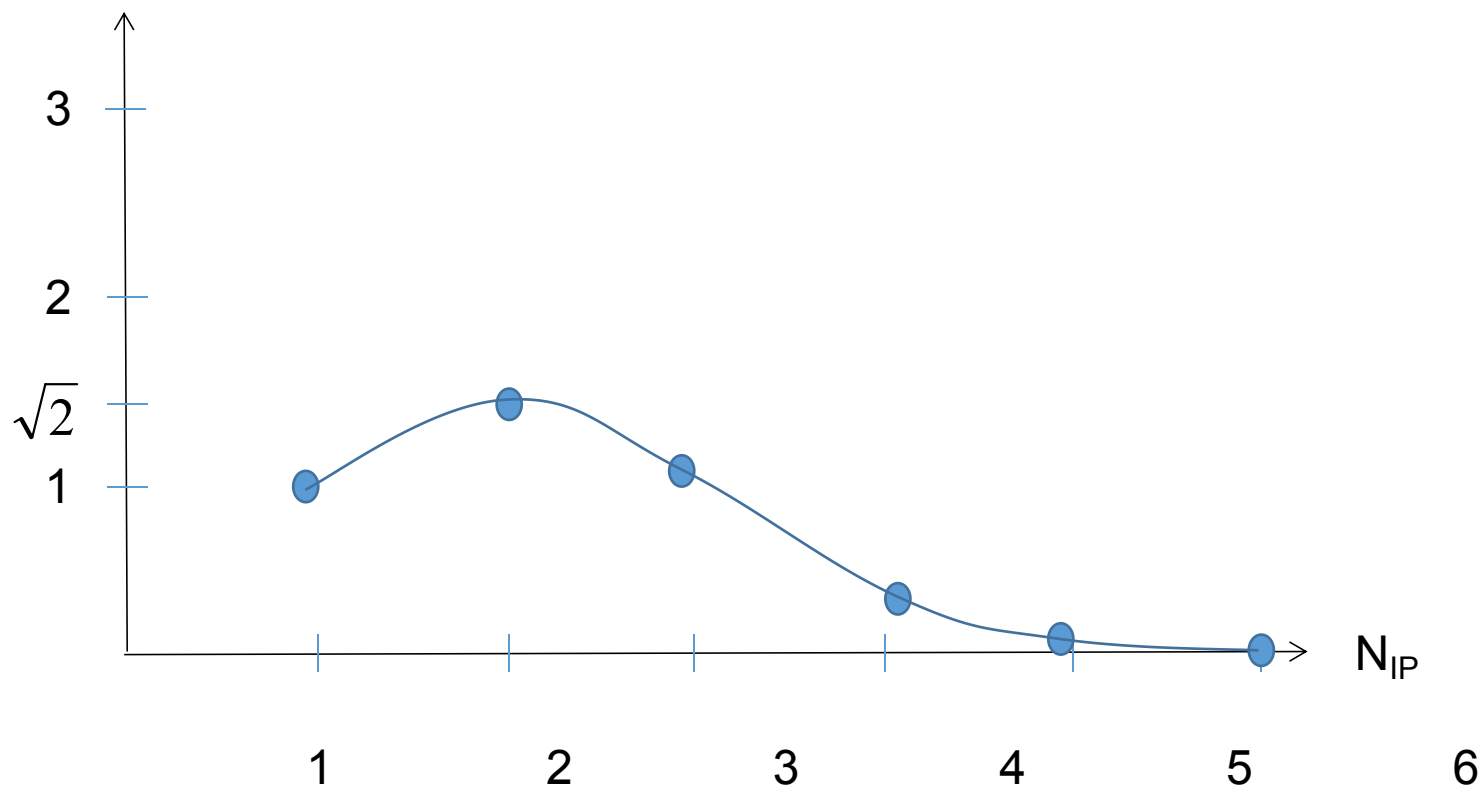
where $\Phi = (\sigma_z/\sigma_x)\phi$ is Piwinski angle.

J. Gao, “Analytical estimation of the effects of crossing angle on the luminosity of an e⁺e⁻ circular collider”, **Nuclear Instruments and Methods in Physics Research A** 481 (2002) 756–759

J. Gao, “Analytical treatment of the nonlinear electron cloud effect and the combined effects with beam-beam and space charge nonlinear forces in storage rings”, **Chinese Physics C** Vol. 33, No. 2, Feb., 2009, 135-144

Discussion on CEPC Interaction Point Number N_{IP}

Sum luminosity of N_{IP} / luminosity of single IP



Space Charge Nonlinear Effects



TESLA COLLABORATION

$$\left(\frac{A_{\text{total},sc,y}(s)}{\sigma_y(s)} \right)^2 = \frac{3}{\sqrt{2}\pi\xi_{sc}}$$

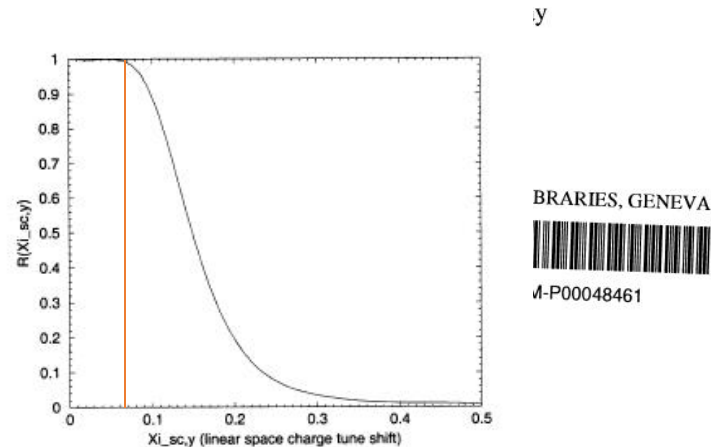
$$\xi_{sc,y} = -\frac{r_e N_e \beta_{av,y}}{2\pi\gamma\sigma_y(\sigma_x + \sigma_y)} \left(\frac{L}{\sqrt{2}\pi\beta^2\gamma^2\sigma_z} \right)$$

J. Gao, "Analytical treatment of the nonlinear electron cloud effect and the combined effects with beam-beam and space charge nonlinear forces in storage rings", **Chinese Physics C** Vol. 33, No. 2, Feb., 2009, 135-144

J. Gao, Theoretical analysis of the limitation from the nonlinear space charge forces to TESLA damping ring **TESLA** 2003-12

Theoretical Analysis on the Limitation from the Nonlinear Space Charge Forces to TESLA Damping Ring

J. Gao



February 2003, TESLA 2003-12

Electron Cloud Nonlinear Effect

$$\xi'_{ec}(s_0) = \frac{r_e N_{ec} \beta_{+,y}(s_0)}{2\pi \gamma_+ \sigma_{+,y}(s_0) (\sigma_{+,x}(s_0) + \sigma_{+,y}(s_0))} \left(\frac{1}{2L_0} \right)$$

$$\left(\frac{A_{ec,y}}{\sigma_{+,y}} \right)^2 \approx \frac{3\sqrt{2}\gamma_+}{\pi r_e \beta_{av,y} \rho_{ec} L}$$

$$\rho_{ec} = \frac{N_{ec}}{2\pi \sigma_{av,+,x} \sigma_{av,+,y} L_0}$$

J. Gao, “Analytical treatment of the nonlinear electron cloud effect and the combined effects with beam-beam and space charge nonlinear forces in storage rings”, **Chinese Physics C** Vol. 33, No. 2, Feb., 2009, 135-144

Combined Beam-Beam, Space Charge, Electron Cloud Nonlinear Effects

$$\mathcal{R}_{ec,y}^2 = \left(\frac{A_{ec,y}}{\sigma_{+,y}} \right)^2 \approx \frac{3\sqrt{2}\gamma_+}{\pi r_e \beta_{av,y} \rho_{ec} L}, \quad \rho_{ec} = \frac{N_{ec}}{2\pi \sigma_{av,+,x} \sigma_{av,+,y} L},$$

$$\mathcal{R}_{total,+,y}^2 = \frac{1}{\frac{1}{\mathcal{R}_{bb,+,y}^2} + \frac{1}{\mathcal{R}_{ec,y}^2} + \frac{1}{\mathcal{R}_{sc,y}^2}},$$

$$\tau_{total,+,y} = \frac{\tau_{+,y}}{2} \left(\mathcal{R}_{total,+,y}^2 \right)^{-1} \exp \left(\mathcal{R}_{total,+,y}^2 \right)$$

J. Gao, “Analytical treatment of the nonlinear electron cloud effect and the combined effects with beam-beam and space charge nonlinear forces in storage rings”, **Chinese Physics C** Vol. 33, No. 2, Feb., 2009, 135-144

Hadron Collider Beam-Beam Limit Formulae (pp)

$$\xi_{h,y,\max} = \frac{H_0 \gamma}{f(x_*)} \sqrt{\frac{r_h}{6\pi R N_{\text{IP}}}}$$

$$H_0 \sim 2845,$$

$$\xi_{h,y,\max} = \frac{H_0}{2\pi f(x_*)} \sqrt{\frac{T_0}{\tau_y \gamma N_{\text{IP}}}}$$

$$f(x) = 1 - \frac{2}{\sqrt{2\pi}} \int_0^x \exp\left(-\frac{t^2}{2}\right) dt$$

$$x^2 = \frac{4f(x)}{\pi \xi_{y,\max} N_{\text{IP}}}$$

$$x_*^2 = \frac{4f(x_*)^2}{H_0 \pi \gamma} \sqrt{\frac{6\pi R}{r_h N_{\text{IP}}}}$$

$f=1$ corresponds electron positron colliders

Machine	N_{IP}	R (m)	γ	$\xi_{y,\max}$	x^*	$f(x^*)$
$Sp\bar{p}S$	3	741	335.75	0.0026	2.187	34.8
TEVATRON	2	682	959	0.0042	2.16	32.5
HERA(p)	2	588	874	0.00426	2.155	32.1
LHC	2	2700	7460	0.005	2.1	28
SSC	2	9824	23400	0.0049	2.116	29.12

J. Gao, “Emittance Growth and Beam Lifetime due to Beam-Beam Interaction in a Circular Collider”, Personal note, 2004 (LAL, Orsay)

J. Gao, “Review of some important beam physics issues in electron positron collider designs”, **Modern Physics Letters A** Vol. 30, No. 11 (2015) 1530006 (20 pages)

J. Gao[†], M. Xiao, F. Su, S. Jin, D. Wang, Y.W. Wang, S. Bai, T.J. Bian, “ANALYTICAL ESTIMATION OF MAXIMUM BEAM-BEAM TUNE SHIFTS FOR ELECTRON-POSITRON AND HADRON CIRCULAR COLLIDERS”, **HF2014 Proceedings** (2014)

On the single bunch longitudinal collective effects in
electron storage rings

J. Gao*

Laboratoire de L'Accélérateur Linéaire IN2P3-CNRS et Université de Paris-Sud, B.P. 34, 91898 Orsay Cedex, France

Received 29 January 2002; received in revised form 14 May 2002; accepted 18 May 2002

Wakefield of a Whole Storage Ring

$$\begin{aligned} W_z(z)(V/C) = & -ak(\sigma_z) \exp\left(-\frac{2z^2}{7\sigma_z^2}\right) \cos\left(\left(1 + \frac{2}{\pi} \operatorname{atan}\left(\operatorname{atan}\left(\frac{Z_i}{2Z_r}\right)\right)\right) \frac{z}{\sqrt{3}\sigma_z}\right. \\ & \left. + \operatorname{atan}\left(\frac{Z_i}{2Z_r}\right)\right), \end{aligned} \quad (25)$$

where σ_z is bunch length, $k(\sigma_z)$ is the total loss factor of the ring, $L(\sigma_z)$ is the total inductance, $a = 2.23$, $Z_i = 2\pi L(\sigma_z)/T_0$, $Z_r = k(\sigma_z)\frac{T_b^2}{T_0}$, $T_0 = 2\pi R_{av}/c$, $T_b = 3\sigma_z/c$,

R_{av} is the average radius of the ring, c is the velocity of light, and $z = 0$ corresponds to the center of the bunch, and all variables are in MKS units.

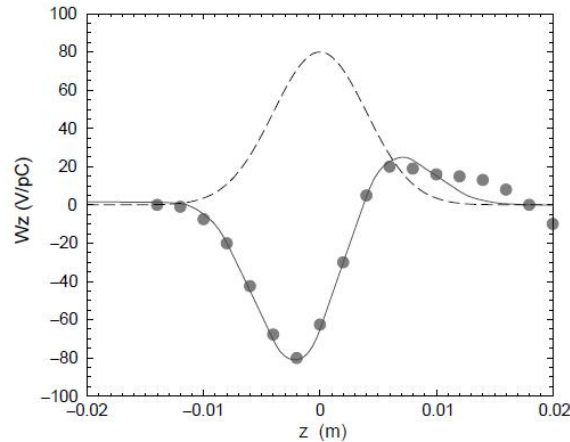


Fig. 1. KEKB low energy ring: the dots and the solid line represent the wake potentials calculated numerically [27] and analytically by using Eq. (2), respectively, with $\sigma_{z0} = 0.004$ m, $L = 22$ nH, and $k(\sigma_{z0}) = 42$ V/pC. The dashed line shows the Gaussian bunch shape with arbitrary units.

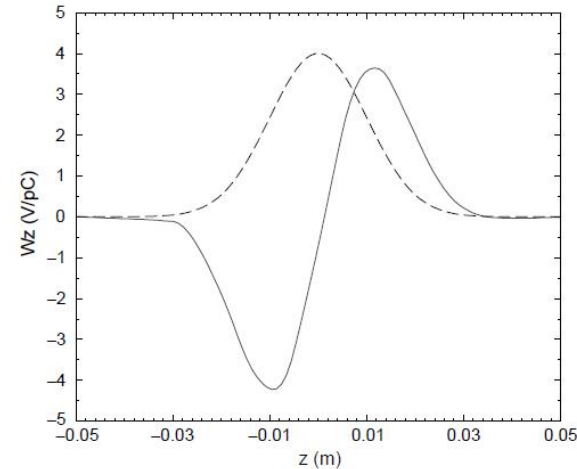


Fig. 3. The solid line represents the total longitudinal wake potential of PEP-II low energy ring with $\sigma_{z0} = 0.01$ m, $L = 83.3$ nH, and $k(\sigma_{z0}) = 2.9$ V/pC. The dashed line shows the Gaussian bunch shape with arbitrary units.

Jie Gao

*Institute of High Energy Physics, Yuquan Road 19, Beijing 100049, P. R. China
 gaoj@ihep.ac.cn*

Bunch Lengthening and Energy Spread Increasing in Storage Ring

According to Ref. 16, bunch lengthening, $R_z = \sigma_z / \sigma_{z0}$, and bunch energy spread increasing, $R_\varepsilon = \sigma_\varepsilon / \sigma_{\varepsilon 0}$, with respect to the bunch current could be estimated as follows:

$$R_z^2 = 1 + \frac{\sqrt{2C} R_{av} R \mathcal{K}_{||,0}^{\text{tot}} I_b}{\gamma^{3.5} (R_z)^\varsigma} + \frac{C (R_{av} R I_b \mathcal{K}_{||,0}^{\text{tot}})^2}{\gamma^7 (R_z)^{2\varsigma}}, \quad (27)$$

where

$$C = \frac{576\pi^2 \epsilon_0}{55\sqrt{3}\hbar c^3}, \quad (28)$$

ϵ_0 is the permittivity in vacuum, \hbar is Planck constant, c is the velocity of light, $\mathcal{K}_{||,0}^{\text{tot}}$ is the total longitudinal loss factor of the whole ring at the natural bunch length, $\sigma_{z,0}$, $I_b = eN_e c / 2\pi R_{av}$, and R_{av} is the average radius of the ring. If SPEAR scaling law⁷ is used (for example), $\varsigma \approx 1.21$ (in fact each machine has its own ς), Eq. (27) can be written as

$$R_z^2 = 1 + \frac{\sqrt{2C} R_{av} R \mathcal{K}_{||,0}^{\text{tot}} I_b}{\gamma^{3.5} R_z^{1.21}} + \frac{C (R_{av} R I_b \mathcal{K}_{||,0}^{\text{tot}})^2}{\gamma^7 R_z^{2.42}}. \quad (29)$$

The procedure to get the information about the bunch lengthening and the energy spread increasing is first to find $R_z(I_b)$ by solving bunch lengthening equation, i.e. Eq. (27), and then calculate energy spread increasing, $R_\varepsilon(I_b)$ ($R_\varepsilon = \sigma_\varepsilon / \sigma_{\varepsilon 0}$), by putting $R_z(I_b)$ into Eq. (30):

$$R_\varepsilon^2 = 1 + \frac{C (R_{av} R I_b \mathcal{K}_{||,0}^{\text{tot}})^2}{\gamma^7 R_z^{2.42}}. \quad (30)$$

Theory of single bunch transverse collective
instabilities in electron storage rings

J. Gao

Laboratoire de L'Accélérateur Linéaire, IN2P3-CNRS, et Université de Paris-Sud, 91405 Orsay cedex, France

Received 27 April 1998; received in revised form 30 June 1998; accepted 6 July 1998

Single Bunch Instability Threshold in a Storage Ring

$$I_{\text{b,zotter}}^{\text{th}} = \frac{F f_s E_0}{e \langle \beta_{y,c} \rangle \mathcal{K}_{\perp}^{\text{tot}}(\sigma_z)} \quad \longrightarrow \quad I_{\text{b,gao}}^{\text{th}} = \frac{F' f_s E_0}{e \langle \beta_{y,c} \rangle \mathcal{K}_{\perp}^{\text{tot}}(\sigma_z)}$$

where f_s is the synchrotron oscillation frequency, E_0 is the particle energy, $\langle \beta_{y,c} \rangle$ is the average vertical beta function at RF cavities, and $\mathcal{K}_{\perp}^{\text{tot}}(\sigma_z)$ is the total transverse loss factor at bunch length σ_z . The

with

$$F' = 4R_{\varepsilon} |\zeta_{c,y}|^{\varepsilon} \frac{v_y \sigma_{\varepsilon 0}}{v_s E_0}.$$

Jie Gao

Institute of High Energy Physics, Yuquan Road 19, Beijing 100049, P. R. China

Single Bunch Emittance Increase due to Transvers Emittances

$$\mathcal{R}_{\epsilon,x} = \frac{\epsilon_{\text{total},x}}{\epsilon_{0,x}} = 1 + \frac{\sigma_X^2 \tau_x \langle \beta_x(s) \rangle}{4T_0 \epsilon_{0,x} \mathcal{R}_{\epsilon,x}^3} \left(\frac{e^2 N_e k_{\perp,x}(\sigma_{z0})}{m_0 c^2 \gamma \mathcal{R}_z^\Theta} \right)^2,$$
$$\mathcal{R}_{\epsilon,y} = \frac{\epsilon_{\text{total},y}}{\epsilon_{0,y}} = 1 + \frac{\sigma_Y^2 \tau_y \langle \beta_y(s) \rangle}{4T_0 \epsilon_{0,y} \mathcal{R}_{\epsilon,y}^3} \left(\frac{e^2 N_e k_{\perp,y}(\sigma_{z0})}{m_0 c^2 \gamma \mathcal{R}_z^\Theta} \right)^2,$$

SINGLE BUNCH LONGITUDINAL INSTABILITIES IN PROTON STORAGE RINGS

J. Gao, LAL, B.P. 34, F-91898 Orsay cedex, France

$$H(I, \theta, t)^* = H(I) + \frac{1}{2} \Delta P^2 T_0 \sum_{k=-\infty}^{\infty} \delta(t - kT_0)$$

$$= H(I) + \frac{(dE)^2 h^2 \eta^2}{2 R_s^2 p_s^2} T_0 \sum_{k=-\infty}^{\infty} \delta(t - kT_0)$$

$$= H(I) + \frac{\mathcal{U}_w^2 h^2 \eta^2 \cos^2 \theta}{2 R_s^2 p_s^2} T_0 \sum_{k=-\infty}^{\infty} \delta(t - kT_0)$$

Microwave instability
starting bunch current

$$I_{b,th} = \frac{R_s p_s}{e \sqrt{|\Omega'|} T_0^2 h |\eta| \mathcal{K}_{//}^{tot}(\sigma_z)}$$

$$|\Omega'| = \frac{1}{\pi^4 |1 - H_b/H_c|} \left(\ln \frac{32}{|1 - H_b/H_c|} \right)^3$$

J. Gao, "Single bunch longitudinal instabilities in proton storage rings", **Proceedings of PAC99**, New York, USA (1999)

where

$$\frac{H_b}{H_c} = \left(\frac{\delta E_b}{\delta E_{max}} \right)^2 = \frac{\pi h |\eta| E_s}{\beta^2 e \hat{V} G(\phi_s)} (\delta E_b)^2$$

$$G(\phi_s) = 2 \cos \phi_s - (\pi - 2\phi_s) \sin \phi_s$$

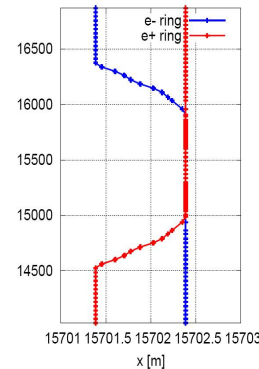
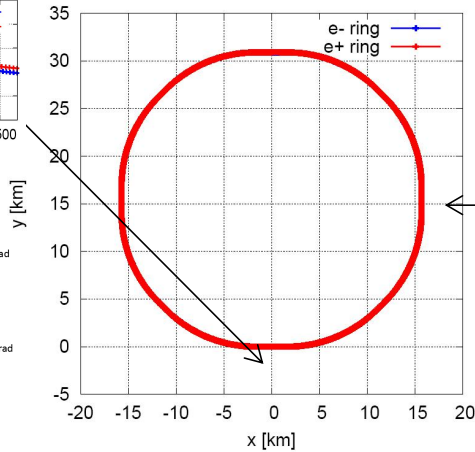
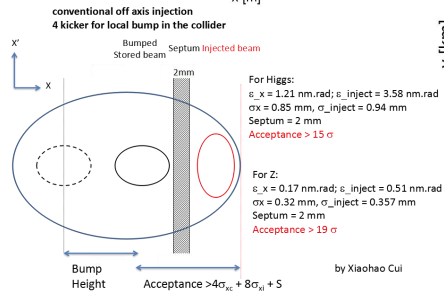
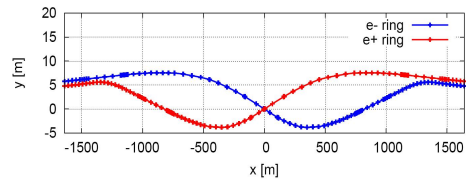
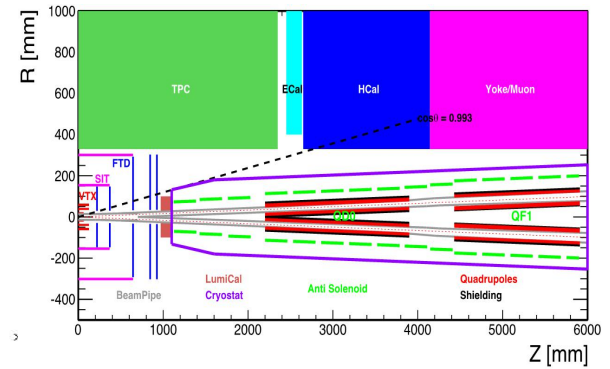
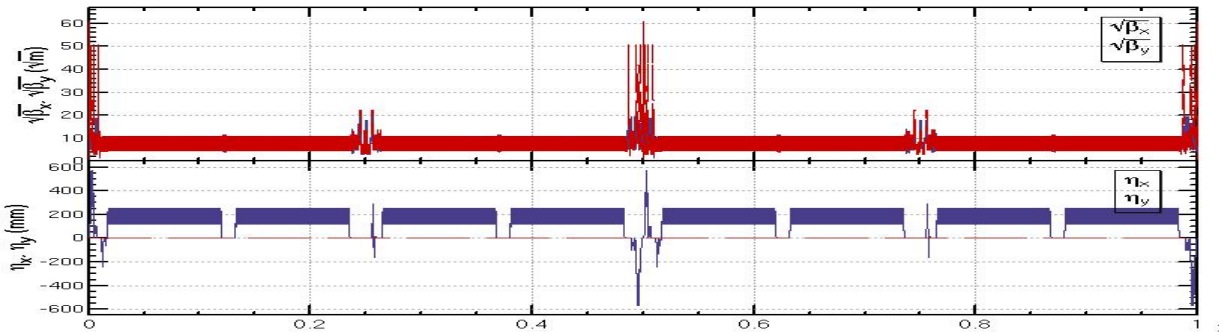
CEPC CDR Parameters

	<i>Higgs</i>	<i>W</i>	<i>Z (3T)</i>	<i>Z (2T)</i>
Number of IPs	2			
Beam energy (GeV)	120	80	45.5	
Circumference (km)	100			
Synchrotron radiation loss/turn (GeV)	1.73	0.34	0.036	
Crossing angle at IP (mrad)	16.5×2			
Piwinski angle	2.58	7.0	23.8	
Number of particles/bunch N_e (10 ¹⁰)	15.0	12.0	8.0	
Bunch number (bunch spacing)	242 (0.68μs)	1524 (0.21μs)	12000 (25ns+10%gap)	
Beam current (mA)	17.4	87.9	461.0	
Synchrotron radiation power /beam (MW)	30	30	16.5	
Bending radius (km)	10.7			
Momentum compact (10 ⁻⁵)	1.11			
β function at IP β_x^*/β_y^* (m)	0.36/0.0015	0.36/0.0015	0.2/0.0015	0.2/0.001
Emittance $\varepsilon_x/\varepsilon_y$ (nm)	1.21/0.0031	0.54/0.0016	0.18/0.004	0.18/0.0016
Beam size at IP σ_x/σ_y (μm)	20.9/0.068	13.9/0.049	6.0/0.078	6.0/0.04
Beam-beam parameters ξ_x/ξ_y	0.031/0.109	0.013/0.106	0.0041/0.056	0.0041/0.072
RF voltage V_{RF} (GV)	2.17	0.47	0.10	
RF frequency f_{RF} (MHz) (harmonic)	650 (216816)			
Natural bunch length σ_z (mm)	2.72	2.98	2.42	
Bunch length σ_z (mm)	3.26	5.9	8.5	
HOM power/cavity (2 cell) (kw)	0.54	0.75	1.94	
Natural energy spread (%)	0.1	0.066	0.038	
Energy acceptance requirement (%)	1.35	0.4	0.23	
Energy acceptance by RF (%)	2.06	1.47	1.7	
Photon number due to beamstrahlung	0.1	0.05	0.023	
Lifetime _simulation (min)	100			
Lifetime (hour)	0.67	1.4	4.0	2.1
F (hour glass)	0.89	0.94	0.99	
Luminosity/IP L (10 ³⁴ cm ⁻² s ⁻¹)	2.93	10.1	16.6	32.1

Lattice of the CEPC Collider Ring and MDI

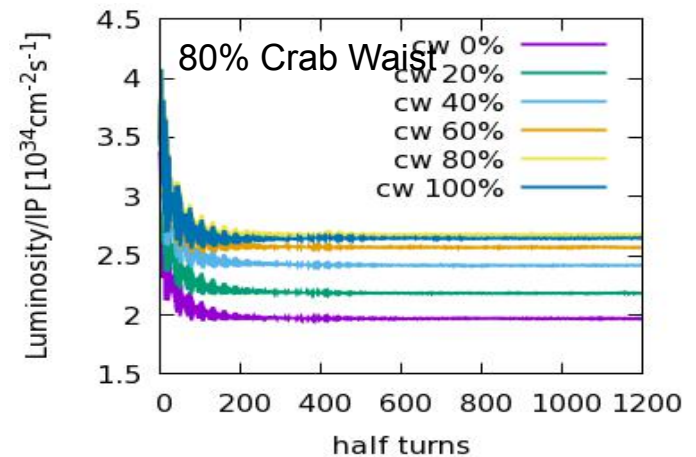
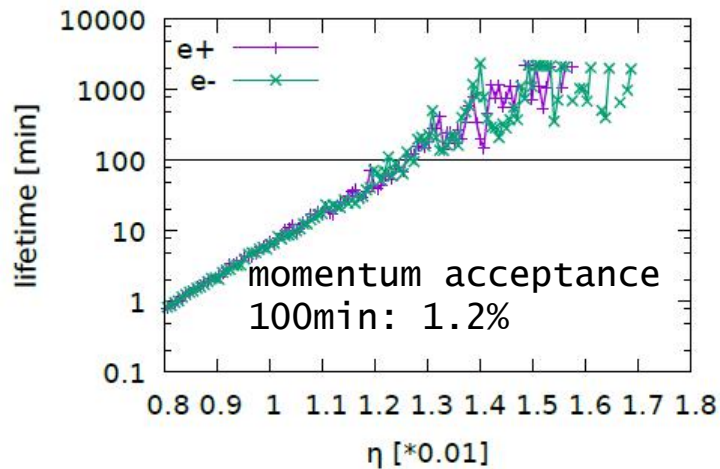
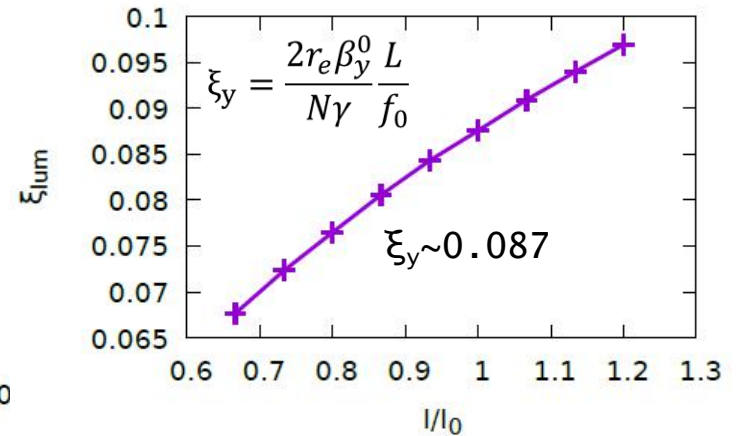
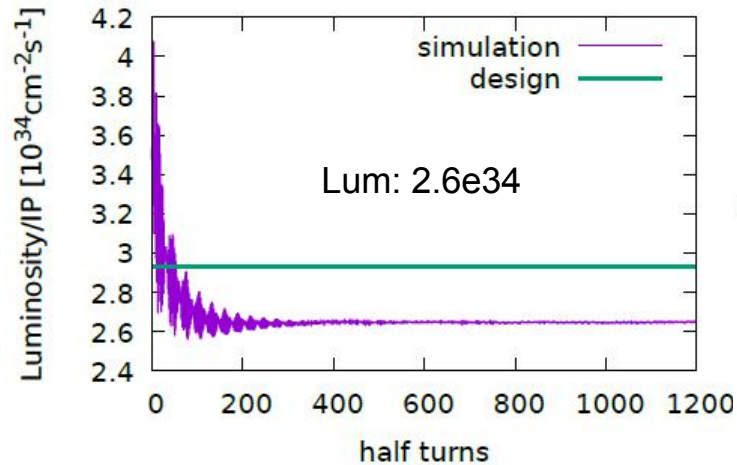
An optics fulfilling requirements of the parameters list, geometry, MDI, background and key hardware

CEPC MDI



MDI parameters	Values
L^* (m)	2.2
Crossing angle (mrad)	33
Strength of QD0 (T/m)	150
Strength of detector solenoid (T)	3.0
Strength of anti-solenoid (T)	7.0

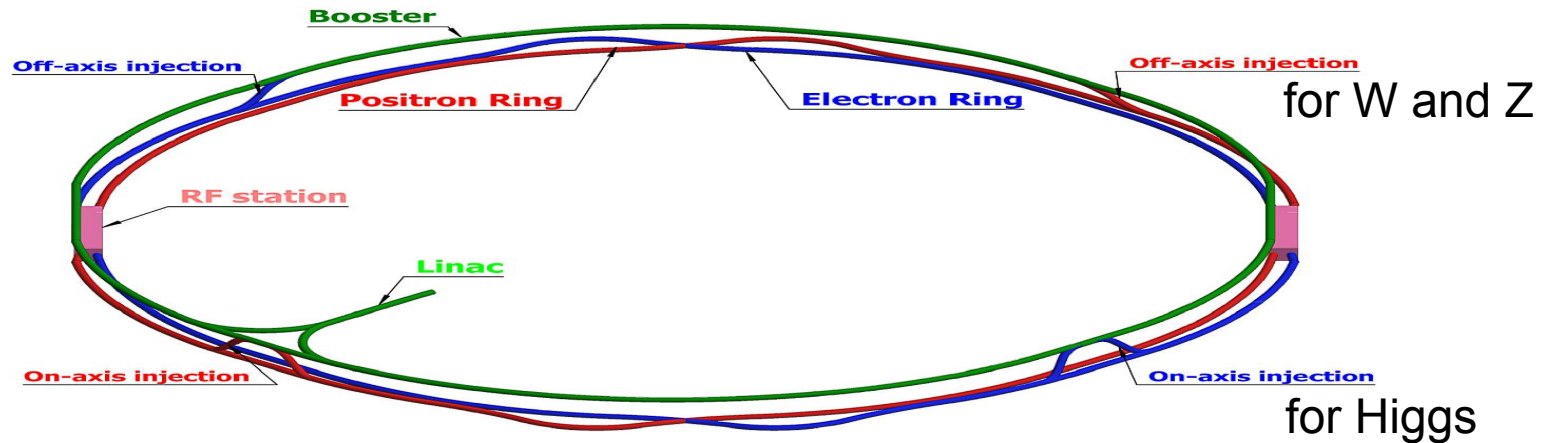
CEPC Beam-Beam Simulation at Higgs



CEPC Collider Ring Requirements on Dynamic Aperture

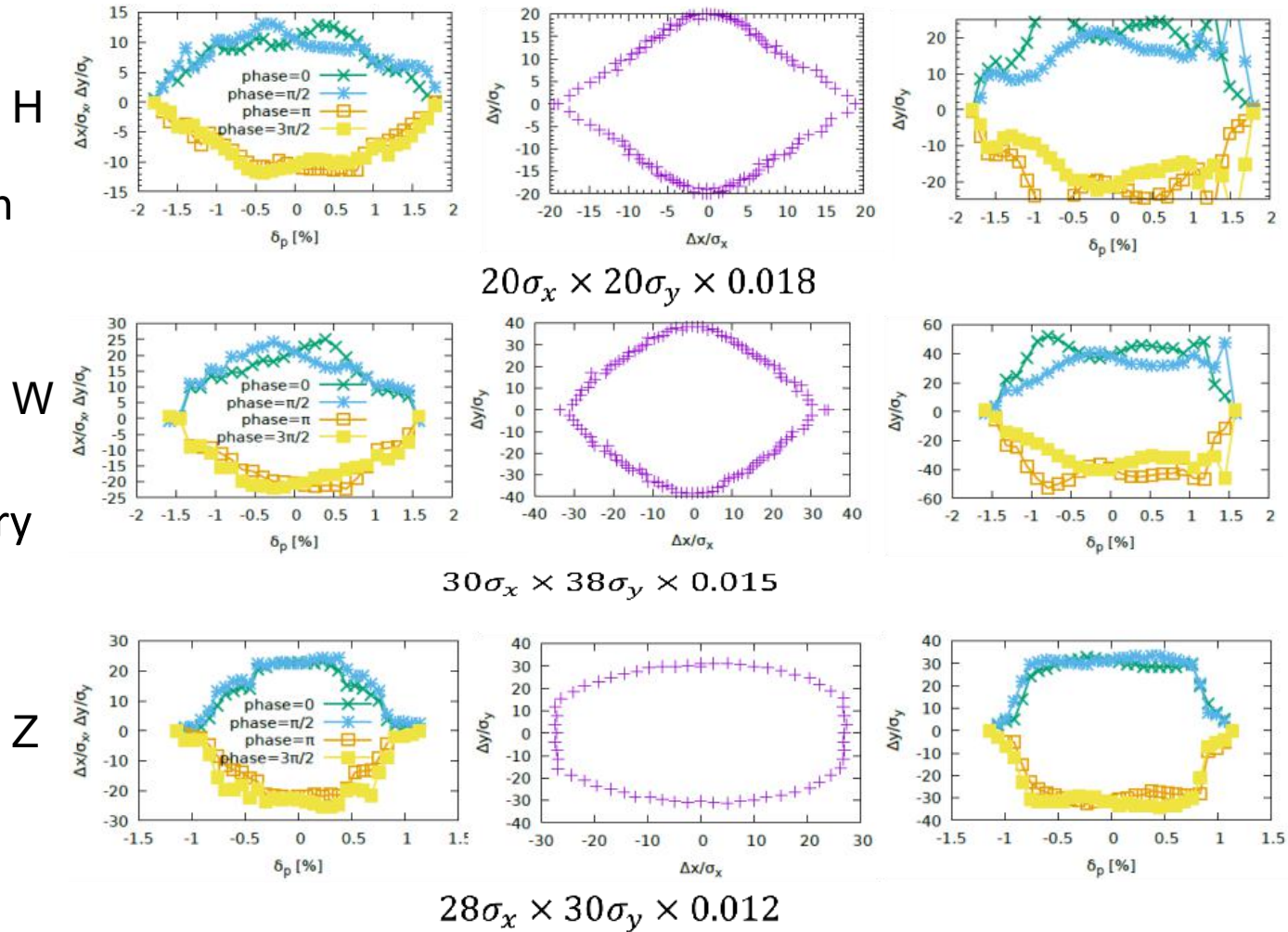
The requirements of dynamic aperture from injection and beam-beam effect to get efficient injection and adequate beam life time:

	Higgs	W	Z
with on-axis injection	$8\sigma_x \times 12\sigma_y \times 1.35\%$	-	-
with off-axis injection	$13\sigma_x \times 12\sigma_y \times 1.35\%$	$15\sigma_x \times 9\sigma_y \times 0.4\%$	$17\sigma_x \times 9\sigma_y \times 0.23\%$



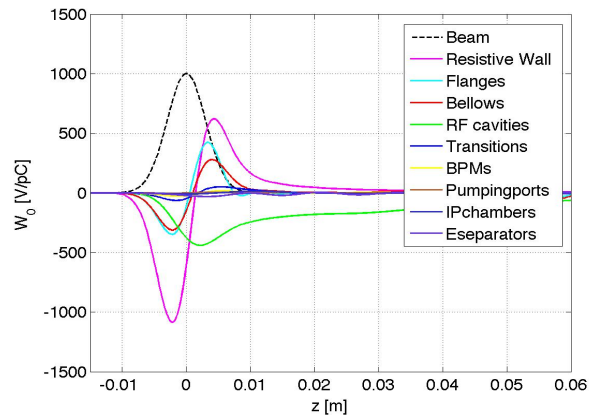
CEPC DA@Higgs,W and Z-pole

- Synchrotron radiation fluctuation is considered
- 100 samples are tracked
- 90% survival boundary is shown



CEPC Collider Ring Impedance Budget

Components	Number	$Z_{ }/n$, m Ω	k_{loss} , V/pC	κ_y , kV/pC/m
Resistive wall	-	6.2	363.7	11.3
RF cavities	336	-1.4	315.3	0.41
Flanges	20000	2.8	19.8	2.8
BPMs	1450	0.12	13.1	0.3
Bellows	12000	2.2	65.8	2.9
Pumping ports	5000	0.02	0.4	0.6
IP chambers	2	0.02	6.7	1.3
Electro-separators	22	0.2	41.2	0.2
Taper transitions	164	0.8	50.9	0.5
Total		10.5	876.8	20.4



Broadband impedance threshold:

Threshold	ttbar	Higgs	W	Z
$ Z_{ }/n _{\text{eff}}$, m Ω	13.6	9.0	8.0	2.1
κ_y , kV/pC/m	81.2	61.6	69.0	38.7

Longitudinal wake at the nominal $\sigma_z = 3\text{mm}$

References

- 1) Matthew Sands, “The physics of electron storage rings: an introduction”, SLAC- 121
- 2) S. Kurukawa, “Basics of electron storage rings”, JASS'02
- 3) J. Gao, “Analytical estimation of the dynamic apertures of circular accelerators”, **Nuclear Instruments and Methods in Physics Research A** 451 (2000) 545-557.
- 4) J. Gao, “Analytical estimation of dynamic apertures limited by the wigglers in storage rings”, **Nuclear Instruments and Methods in Physics Research A** 516 (2004) 243–248
- 5) J. Gao, “Analytical estimation of the beam–beam interaction limited dynamic apertures and lifetimes in e+e- circular colliders”, **Nuclear Instruments and Methods in Physics Research A** 463 (2001) 50–61
- 6) J. Gao, ON PARASITIC CROSSINGS AND THEIR LIMITATIONS TO E+E– STORAGE RING COLLIDERS, **Proceedings of EPAC 2004**, Lucerne, Switzerland, p. 671-673 (2004)
- 7) J. Gao, “Analytical treatment of the nonlinear electron cloud effect and the combined effects with beam-beam and space charge nonlinear forces in storage rings”, **Chinese Physics C** Vol. 33, No. 2, Feb., 2009, 135-144

- 8) J. Gao, "Analytical estimation of the effects of crossing angle on the luminosity of an e+e- circular collider", **Nuclear Instruments and Methods in Physics Research A** 481 (2002) 756–759
- 9) J. Gao, "Analytical treatment of the nonlinear electron cloud effect and the combined effects with beam-beam and charge nonlinear forces in storage rings", **Chinese Physics C** Vol. 33, No. 2, Feb., 2009, 135-144
- 10) J. Gao, Theoretical analysis of the limitation from the nonlinear space charge forces to TESLA damping ring, **TESLA 2003-12**
- 11) J. Gao, "Emittance Growth and Beam Lifetime due to Beam-Beam Interaction in a Circular Collider", **Personal note**, 2004 (LAL, Orsay)
- 12) J. Gao, "Review of some important beam physics issues in electron positron collider designs", **Modern Physics Letters A** Vol. 30, No. 11 (2015) 1530006 (20 pages)
- 13) J. Gao†, M. Xiao, F. Su, S. Jin, D. Wang
Y.W. Wang, S. Bai, T.J. Bian, "ANALYTICAL ESTIMATION OF MAXIMUM BEAM-BEAM TUNE SHIFTS FOR ELECTRON-POSITRON AND HADRON CIRCULAR COLLIDERS", **HF2014 Proceedings** (2014)
- 14) M. Xiao and J. Gao, "ANALYTICAL ESTIMATIONS OF THE DYNAMIC APERTURES OF BEAMS WITH MOMENTUM DEVIATION AND APPLICATION IN FFAG", WEPEA022 **Proceedings of IPAC2013**, Shanghai, China, p. 2546-2548
- 13) J. Gao, "Single bunch longitudinal instabilities in proton storage rings", **Proceedings of PAC99**, New York, USA (1999)

- 14) J. Gao† , M. Xiao, F. Su, S. Jin, D. Wang
Y.W. Wang, S. Bai, T.J. Bian, “ANALYTICAL ESTIMATION OF MAXIMUM BEAM-BEAM
TUNE SHIFTS FOR ELECTRON-POSITRON AND HADRON CIRCULAR
COLLIDERS”, **HF2014 Proceedings** (2014)
- 15) M. Xiao and J. Gao, “ANALYTICAL ESTIMATIONS OF THE DYNAMIC APERTURES
OF BEAMS WITH MOMENTUM DEVIATION AND APPLICATION IN FFAG”, WEPEA022
Proceedings of IPAC2013, Shanghai, China, p. 2546-2548
- 16) J. Gao, “Single bunch longitudinal instabilities in proton storage rings”, **Proceedings of
PAC99**, New York, USA (1999)
- 17) J. Gao, “Theory of single bunch transverse collective
instabilities in electron storage rings”, **Nuclear Instruments and Methods in Physics
Research A** 416 (1998) 186—188
- 18) J. Gao, “On the scaling law of single bunch transverse instability
threshold current vs. the chromaticity in electron storage rings”, **Nuclear Instruments and
Methods in Physics Research A** 491 (2002) 346—348
- 19) J. Gao, “Analytical estimation of dynamic apertures limited by the
wigglers in storage rings”, **Nuclear Instruments and Methods in Physics Research A** 516
(2004) 243—248
- 20) J. Gao, “Analytical estimation of the effects of crossing angle on the
luminosity of an e^+e^- circular collider”, **Nuclear Instruments and Methods in Physics
Research A** 481 (2002) 756—759
- 21) J. Gao, “On the single bunch longitudinal collective effects in
electron storage rings”, **Nuclear Instruments and Methods in Physics Research A** 491
(2002) 1—8
- 22) J. Gao, “Analytical treatment of some selected problems in particle accelerators”, LAL/RT
03-04, 2003

- 23) CEPC-SppC CDR <http://cepc.ihep.ac.cn/preCDR/volume.html>.
- 24) CEPC-SppC Progress Report <http://cepc.ihep.ac.cn/Progress%20Report.pdf>.
- 25) J Gao, 2017 2017 Int. J. Mod. Phys. A 32 1746003.
- 26) J Gao, A milestone year for Higgs factories in Aisa. ILC Newsline, 2018, March 1 (<http://newsline.linearcollider.org/2018/03/01/2018milestoneyearasia/>)
- 27) J Gao, China's bid for a circular electron-positron collider. CERN Courier, 2018, June 1, (<http://cerncourier.com/cws/article/cern/71537>)

Some references could be down loaded from following website

<http://indico.ihep.ac.cn/event/7393/>